Seasonal impact of submesoscale eddies on the ocean heat budget near the sea ice edge

Lily Greig[1,a] and David Ferreira[2]

[1]Department of Mathematics, University of Reading, Whiteknights Campus, Reading RG6 6UR, UK
[2]Department of Meteorology, University of Reading, Whiteknights Campus, Reading RG6 6UR, UK
[a]Now at: Centre for Environment, Fisheries and Aquaculture Science (Cefas), Pakefield Road, Lowestoft, NR33 0HT, United Kingdom.
Correspondence: lily.greig@cefas.gov.uk

Abstract. Oceanic submesoscale mixed layer eddies (SMLEs), with horizontal scales of 0.1-10 km, are not captured in climate models. SMLEs energized in the marginal ice zone (MIZ) have been shown to be of importance to sea ice melt rates in summer and to sea ice transport through notably a dynamical coupling with sea ice. Here our focus is on the thermodynamical coupling, which has received comparatively little attention. We aim to quantify, for the first time, the impact of eddies on both sea ice and the heat budget in the MIZ, contrasting different seasons and different background stratifications.

To this end, we set up SMLE-resolving simulations of the ocean mixed layer (ML) near the ice edge using the MITgcm, representing a lead or the MIZ. We isolate the effect of eddies by comparing 3D simulations with eddies to 2D (latitude-depth) simulations without eddies.

In summer (i.e., melting conditions) and regardless of the background stratification, SMLEs act as a heat pump from the atmosphere over the open ocean to the sea ice. On average over a season, SMLEs triple the meridional heat transport to the ice covered region, increase melting over their meridional extent, and trigger a positive radiative feedback by increasing shortwave absorption over the thinner ice. These changes are in the range 20-60% for reasonable choices of shortwave forcing and initial ice thickness. In winter (i.e., freezing conditions), SMLEs have a relatively small impact on sea ice growth due to compensation between vertical and horizontal eddy heat transports. However, they reduce ML deepening by 80/50% in the open/ice-covered ocean. Overall, our results reveal up to order one impacts of SMLEs on the heat and sea ice budgets in the MIZ, which will require the development of a SMLE parameterization tailored for polar regions.

1 Introduction

Sea ice is a critical component of the climate system. This is because of its high albedo and the way it mediates air-sea heat and momentum exchanges in polar regions. Predicting the evolution of the sea ice cover in both the Arctic and Antarctic is extremely challenging due to a lack of understanding of the climate processes influencing it (IPCC, 2023; Stroeve

et al., 2012). Ocean heat content and transport have been shown to be a major regulator of the position of the sea ice edge ~~(Bitz et al., 2005; Aylmer et al., 2024, and references therein)~~as well as a leading driver of recent rapid Antarctic sea ice loss (Purich and Doddridge, 2023; Bitz et al., 2005; Aylmer et al., 2024, and references therein). This oceanic influence can be direct from the ocean to the sea ice but can also be mediated by air-sea exchanges near the ice edge (Aylmer et al., 2022). Aylmer et al. (2022) show~~for instance~~ , for instance, that increased ocean heat transport toward the Arctic is associated with increased heat release equatorward of the ice edge and increased atmospheric energy transport toward the central ice pack. As the Arctic sea ice cover is becoming ~~increasingly~~ more and more dominated by the Marginal Ice Zone (MIZ) – the region that lies between pack ice and open ocean (Vichi, 2022; Rolph et al., 2020; Frew et al., 2025), it is likely that such ocean-atmosphere-sea ice interactions will become increasingly important in regulating the sea ice extent.

~~Building knowledge of the oceanic mechanisms at play here is critical to making progress in our understanding (Docquier and Koenigk, 2~~ ~~. Both the~~ In particular, both the MIZ and leads (cracks in the sea ice cover) represent areas of strong lateral density gradients in the upper ocean due to spatial heterogeneity of buoyancy forcing to the ocean. These upper ocean fronts lead, through baroclinic instability, to the energisation of submesoscale ~~processes (Swart et al., 2020; Horvat et al., 2016; Manucharyan and Thompson, 2017)~~ ~~.~~

~~The oceanic submesoscale is typically defined by processes with~~ eddies (Haine and Marshall, 1998; Fox-Kemper et al., 2008; Swart et al ~~. While a handful of spottings from space in the 1960s first revealed their existence, modern observations and high-resolution~~ modelling suggest that these submesoscale mixed layer eddies (SMLEs) are ubiquitous in the world ocean (Munk et al., 2000). SMLEs typically have length scales of the order of 100 metres to 10 kilometres, and time scales of days to weeks, i.e., Rossby number of order 1. ~~These processes are associated with the weakly stratified~~ Because of the weak stratification of the ocean mixed layer (ML), ~~and~~ they are also associated with Richardson numbers of order 1. ~~These processes were first observed from space in the 1960s and, due to further observations since, are now regarded to be ubiquitous in the ocean (Munk et al., 2000) . Amongst the submesoscale dynamics are submesoscale mixed layer eddies (SMLEs). These baroclinic SMLEs develop through the baroclinic instability in the ML (Haine and Marshall, 1998; Fox-Kemper et al., 2008). Due to their small scales, SMLEs are not resolved in global climate models, yet they are a potentially important process to take into account at global scales (Hewitt et al., 2022). SMLEs have the potential to set~~ The importance of SMLEs cascades to the large-scale due to their influence on stratification, ML depth (MLD)~~and to influence the stratification of the surface ocean and~~ , air-sea interactions~~(Hosegood et al., 2006; Fox-Kemper et al., 2011; Thompson et al., 2016; McWilliams, 2016; Taylor and Thompson, 2023)~~ , and biogeochemical processes (Hewitt et al., 2022; Hosegood et al., 2006; Fox-Kemper et al., 2011; Thompson et al., 2016; McWilliams, .

In the last decade or so, ~~SMLEs~~ submesoscale dynamics in polar regions ~~have~~ has received increasing attention. Observational campaigns ~~initially sought to find evidence for~~ revealed the presence of submesoscale fronts and flows in ~~polar regions, which were found in abundance (Timmermans et al., 2012; Timmermans and Winsor, 2013; Giddy et al., 2020; Swart et al., 2020) . One focus of such campaigns has been to understand the interaction of SMLEs with their environment, which, critically, in polar regions includes interactions with sea ice . Evidence has been found that the seasonal cycle of submesoscale eddy heat fluxes and their interaction with winds is partly established by~~ abundance in polar regions (Timmermans et al., 2012; Timmermans and Wins

. They also provided evidence for the impact of the sea ice cover on SMLE dynamics, for example by modulating the interaction with surface winds over the seasonal cycle ~~of the sea ice cover (Giddy et al., 2020; Swart et al., 2020)~~(Giddy et al., 2021; Swart et al., 2020)
.

~~Alongside these observational campaigns, numerical modelling studies have brought to light different mechanisms of~~ SMLE-sea ice interaction ~~. During the melt season, SMLEs have the potential to transport heat under ice and influence lateral melt rates. As a result of this interaction, the dependence of floe melt rates on floe size extends in the range 1-50 km (smaller floes, which have a larger perimeter for the same sea ice volume, melting faster), a much larger scale range than previously thought (Horvat et al., 2016; Horvat and Tziperman, 2018). Eddies~~mechanisms have been further investigated in numerical modelling studies, though the emphasis has been largely on mechanical interactions. SMLEs, if energised in the MIZ, could mechanically trap sea ice floes and advect them into warmer waters, resulting in increased ice melt (Manucharyan and Thompson, 2017) ~~, although the details of the trapping mechanism remain debated (Gupta and Thompson, 2022). In leads , ice-ocean stresses were found to have a limited influence on the eddy development, whilst another study found that in partially sea~~ although this effect is significantly modulated when thermodynamic interactions are also included (Gupta and Thompson, 2022). In leads and partially sea ice-covered ~~regions~~ regions, the ocean-ice friction could influence SMLE development. However, studies find somewhat contrasting results: while it was suggested that ocean-ice friction could reduce eddy overturning by 40%~~(Cohanim et al., 2021; Shrestha and Manucharyan, 2022)~~, other studies showed that the influence of friction on eddy development is limited (Cohanim et al., 2021; Shrestha and Manucharyan, 2022; Brenner et al., 2023).

~~The~~ Horvat et al. (2016) and Horvat and Tziperman (2018) focused on thermodynamic interactions to show that, during the melting season, SMLEs have the potential to alter lateral melt rates by laterally transporting heat under ice. This process extends the dependence of floe melt rates on floe size up to 50 km - a much larger scale than previously thought when not considering SMLEs.

However, the thermodynamic interactions of SMLEs with sea ice cover and atmosphere remain under-explored. Observations and numerical modelling (e.g. Gupta and Thompson, 2022; Swart et al., 2020) suggest that the impacts of SMLEs ~~in polar regions are influenced by~~ should depend on the background oceanic and atmospheric ~~environmental conditionsof MIZs (winds, ocean stratification, shortwave radiation reaching ocean surface) (Gupta and Thompson, 2022; Swart et al., 2020). These background conditions set the parameters that control SMLE fluxes (MLD, lateral density gradient) and therefore could control the eddy feedback onto these background properties too~~conditions, and therefore should vary seasonally and regionally. For example, the ~~eddy length scale is set by the ML Rossby radius of deformation, which scales with the ambient stratification (Thomas et al., 2008). The horizontal scale of SMLEs whose development is driven by brine release as sea ice forms within leads has been shown to scale directly with the salt input, also indicating the importance of surface forcing for the SMLE field (Matsumura and Hasumi, 2008)~~impact of SMLEs on the polar environment is expected to differ between Arctic and Antarctic as the latter tends to exhibit a weaker upper ocean stratification than the former.

~~The prevalence and importance of SMLEs is expected to increase under global warming and with the increasing~~

SMLEs are not resolved in global climate models, which rely on parameterizations. As the width of the Arctic MIZ ~~(Manucharyan and Thompson, 2022). The impact of these eddies on air-sea heat fluxes remains largely unknown, as is the~~

dependence of the magnitude of these impactson sea ice and other climate variables that depend strongly on the season and background stratificationincreases under global warming, the importance of SMLEs in polar regions is expected to grow (Manucharyan and Thompson, 2022). Robust parameterizations of SMLEs in polar regions requires first solid understanding of their impacts, and then potentially, adaptations of parametrizations to polar conditions.

In the present study, we isolate the thermodynamic impacts of eddies in polar regions, as it was less of a focus in most previous studies which has been the focus of a limited number of previous studies (such as the afore-mentioned Horvat et al. (2016); Horvat). Specifically, our aim is to understand the thermodynamic impact of SMLEs on sea ice, air-sea fluxes, and MLD in the vicinity of the sea ice edge (representing the MIZ or a lead). We also expand on previous work by contrasting how the impact of SMLEs is modulated by seasons (sea ice growth versus melting conditions), background stratification (Arctic versus Antarctice.g., Arctic-like versus Antarctic-like temperature and salinity profiles), and initial MLD. To this end, we compare 3D submesocale-resolving simulations with 2D (latitude-depth) simulations without eddies. This allows us to quantify eddy impacts through sea ice volume changes and heat budget terms, which we link to the eddy-induced overturning streamfunction (Fox-Kemper et al., 2008). We show that SMLEs have a leading order impact on the evolution of the ocean-ice state although the mechanisms are radically different between seasons. We also find that the background stratification is a key control in winter conditions but not in summer conditions.

The structure of the paper is as follows. In section 2, the experimental set-up and the analysis methods used are described. Section 3 gives the results, of which there are four subsections, Arctic summer (3.1), Arctic winter (3.2), Antarctic sensitivity to background stratification (3.3), and further sensitivity analysis (3.4). For Arctic summer, first, the development of SMLEs is described (section 3.1.1). Next in section3.1.2 the influence of eddies on sea ice and air-sea fluxes is explored through heat budgets and through comparisons between 3D simulations with eddies and 2D simulations (no zonal variation) without eddies. In section ?? the eddy dynamics are described through the residual-mean theory framework. The same order is followed for Arctic winter in sections 3.2.1-?? and in ?? the eddy impact to MLD is investigated. The The key results are summarised in section 4, including the difference in eddy impact on sea ice, ML heat storage, air-sea flux and MLD depending on season and background stratificationis discussed in section 4, where the key results are also summarised.

2 Materials and Methodsmethods

2.1 Model set-up

In this study, the Massachussetts Institute of Technology general circulation model (MITgcm) is employed in hydrostatic mode (Marshall et al., 1997b, a). The model set-up is developed from and based on that used by Horvat et al. (2016). Horvat et al. (2016). The domain is a hydrostatic reentrant zonal channel on an f-plane f-plane and is 75 km in both horizontal directions with walls on the northern and southern boundaries (Fig. 1a). The horizontal grid spacing is 250 m and the vertical grid spacing is 2.5 m over the top 75 m, increasing by 20% at each subsequent grid point to atotal depth of 538 m. A thermodynamic sea ice package is usedsuch that the sea ice advection by the ocean is switched off. In addition there is a free-slip boundary on the ice-ocean interface. The northern horizontal extent of the domain is initially covered with 1 m thick

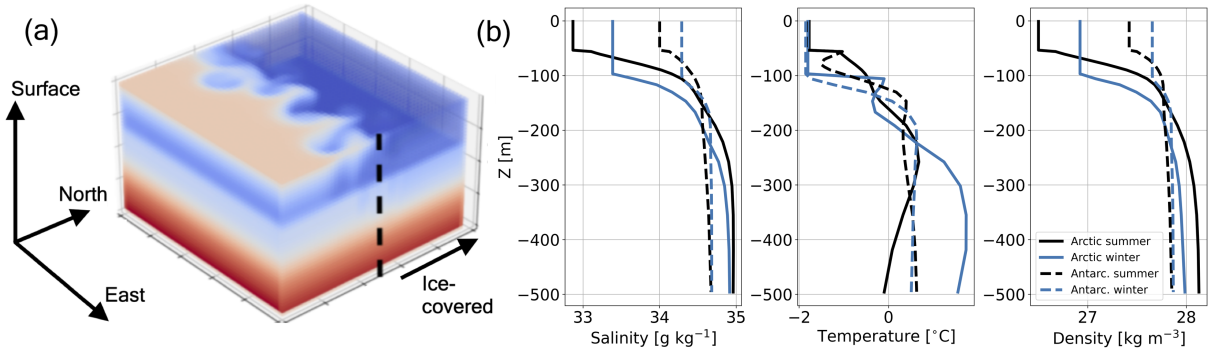

Figure 1. (a) Arctic summer set-up (temperature field), where the northern region is initially ice-covered and the southern region is ice-free. (b) initial salinity, temperature and density profiles for ~~the four main experiments:~~ Arctic/~~Antarctic~~ Antarctic-like stratification (solid/dashed lines) and for summer/winter (black/blue lines)~~conditions~~.

~~sea ice, and the southern half is open ocean. Further~~ , and there is no wind forcing. ~~Vertical mixing is represented by the K-profile parameterisation mixing scheme (Large et al., 1994). Under summer conditions, a Smagorinsky viscosity scheme is used, with the Smagorinsky scaling coefficient set to 2. In winter conditions, vertical mixing and vertical velocities are much more intense than in the summer due to the large surface buoyancy loss (e.g., sensible heat loss, brine rejection). This requires higher viscosity to maintain numerical stability. To avoid damping all motions, we employed a horizontal eddy viscosity of 50 $m^2\ s^{-1}$ on the divergent component of the flow and of 1 $m^2\ s^{-1}$ on the rotational component of the flow in winter simulation. In addition, a small horizontal diffusivity of 1 $m^2\ s^{-1}$ is also used in winter simulations. An atmospheric boundary model evolves the atmospheric temperature in response to air-sea/air-ice fluxes (Deremble et al., 2013). There is no evaporation or precipitation between ocean and atmosphere.~~ More details of the model set-up are provided in A1.

A 2-dimensional ~~version ($y - z$ only~~configuration (latitude-depth only), but otherwise identical to the 3D ~~simulation) of this~~ configuration is also set up. In this configuration, named "no eddies" hereafter, ~~SMLE~~ SMLEs are unable to develop because zonal variations and baroclinic instability are suppressed. Comparison between the ~~2d and 3d~~ 2D and 3D simulations provides measures of the impact of eddies (see section 2.2).

~~Four main experiments are carried out representing combinations of Arctic/Antarctic conditions and~~ The two main experiments represent summer and winter conditions with an Arctic-like initial stratification (we hereon refer to these two experiments as the Arctic summer and Arctic winter experiments, see sections 3.1-3.2). Furthermore, to test the sensitivity to background stratification, two summer/winter ~~conditions. The Antarctic and Arcic conditions are distinguished through the choices of the~~ experiments are carried out using Antarctic-like initial temperature and salinity profiles ~~. These~~ (section 3.3). The initial temperature and salinity profiles for these four experiments are taken from ~~Good et al. (2013),~~ the EN4.2.1 ocean ~~data~~ dataset (Good et al., 2013) near the ice edge. ~~The single 2016 profiles~~ Specifically, for the Arctic, profiles were taken at (84°N, 0°E) ~~were taken for Arctic summer (July)~~ in July and (83°N, 0°E) ~~for winter (January). Antarcticinitial temperature and salinity~~ in January in 2016. For the Antarctic, profiles were taken ~~near the ice edge~~ at (63 °S, 0°E) ~~for the winter ((July)~~ in July and

(69 °S, 0°E) ~~for the summer (January)~~in January. The ML temperature in all initial profiles is set to freezing point and for the winter/summer the initial MLD is 100/55 m. ~~Initial~~ Sensitivity analysis to these initial MLD values is discussed in section 3.4. The initial temperature and salinity profiles are shown in Fig. 1 and are horizontally uniform over the whole domain.

The atmospheric ~~forcing values~~ forcings and initial MLD values are (loosely) based on the European Centre for Medium-Range Weather Forecasts' atmospheric reanalysis version 5 (ERA5) ~~data from~~ and ocean reanalysis system 5 (ORAS5) near the ice edge at 0°E in 2016. ~~The~~ For the summer experiments, the atmospheric temperature T_a is prescribed at -10 °C. A uniform shortwave forcing ($F_{SW,d}$) of 210 W m^{-2} and longwave forcing ($F_{LW,d}$) of 220 W m^{-2} are applied at the ocean surface. ~~In winter~~ For the winter experiments, we use T_a=-5 °C, $F_{SW,d}$=50 W m^{-2}, and $F_{LW,d}$=175 W m^{-2}, which can be considered gentle winter conditions.

We emphasize that the initial conditions and surface forcings are not meant to capture specific observed conditions, but rather to test the sensitivity of SMLEs to typical conditions found in the Arctic/Antarctic MIZs in winter/summer times.

From the prescribed atmopsheric conditions, the net surface heat flux, Q_{net}, is thus given (for the open ocean) ~~is thus given by:~~ by:

$$Q_{net} = F_{LW,d} - \epsilon\sigma T^4 + F_{SH} + F_{SW,d}, \quad (1)$$

where $F_{LW,d}$ is the downwelling longwave radiation, $\epsilon\sigma T^4$ is the outgoing longwave radiation, ϵ is the ocean emissivity, σ is the Stefan-Boltzmann constant, and the net longwave radiation $F_{LWnet} = F_{LW,d} - \epsilon\sigma T^4$. F_{SH} is the sensible turbulent heat flux~~and $F_{SW,d}$ is the downwelling shortwave radiation~~, and F_{SW} hereafter will refer to the net shortwave radiation absorbed by the ocean (including the ocean albedo effect).

For the ice-covered ocean, the surface heat flux is computed using the 3-layer sea ice model of Winton (2000) (see also MITgcm contributors (2025)), in which the energy balance at the ocean/ice interface is between the conductive heat flux through ice, the shortwave penetration through ice and the latent heat of melting/freezing.

All simulations are run for 110 days to roughly match the length of the season. To allow instabilities to develop in the 3D model, the initial temperature was seeded with small-amplitude white noise between 0 and 0.05 °C, so that the mean initial temperature in the mixed layer is slightly (+0.025 °C) above freezing. Results were found to ~~not be sensitive~~ be insensitive to the magnitude of the noise ~~in the initial temperature field~~ (tests were carried out for noise $\pm$ 0.0125-0.8 °C).

2.2 Residual-mean framework

~~The time-mean Eulerian Overturning Streamfunction (EOS) is calculated via zonal integration at a fixed height of the meridional velocity field:~~

$$\overline{\psi}(y,z) = -L_x \int_{H_d}^{z} \overline{v}(y,z')\mathrm{d}z',$$

~~where H_d indicates the ocean bottom, L_x is the zonal extent of the domain, and $\overline{v}$ is the time and zonally-averaged meridional velocity field, which removes eddy effects.~~

Following Abernathey et al. (2011), the isopycnal streamfunction is defined as:

$$\psi_{iso}(y,\rho) = \int_X \int_{\rho_d}^{\rho} (vh)\mathrm{d}\rho'\mathrm{d}x,$$

where $h = \frac{-\partial z}{\partial \rho}$ is To explore the SMLE dynamics, we adopt a residual-mean framework (e.g., Marshall and Radko, 2003). In essence, the framework captures that the total averaged transport within a density layer thickness, ρ_d is the density of the deepest isopycnal, and ρ' is a dummy variable of integration. To calculate ψ_{iso}has two components. First, there is the product of the averaged meridional velocity $\overline{v}$ and averaged layer thickness (in metres) $\overline{H_\rho}$, $\overline{v}\,\overline{H_\rho}$. The second component is the eddy component $\overline{v'H'_\rho}$, where dashes represent the departures from the average. Overall, we have $\overline{vH_\rho} = \overline{v}\,\overline{H_\rho} + \overline{v'H'_\rho}$. That is, the *layers* package in MITgcm is used. It calculates the layer transport $vH_\rho(x,y,\rho,t)$ online (at every time step), where $H_\rho(x,y,\rho,t)$ is the thickness of a density layer bin in metres(time averaging can be done later on) . These density layer bins are chosen by the user at the start of the simulation. The full range of density bins chosen must cover the full range of ocean densities included in the simulation as well as their variation in time. $\psi_{iso}(y,\rho)$ in Eqn. (A2) iscalculated by taking the cumulative sum of $\overline{vH_\rho}(y,\rho)$ (total (residual-mean) transport carrying, say, temperature is the sum of a Eulerian mean flow contribution and an eddy-induced contribution.

In practice here, following Abernathey et al. (2011) and others, we will work with meridional overturings (in Sverdrups) in the sum was taken from the deepest isopycnal upwards). In this way, the meridional velocity v is integrated with respect to isopycnal layers rather than fixed vertical levels as in $\overline{\psi}(y,z)$. Ideally, $\psi_{iso}(y,\rho)$ should be robust to the choice of density bins used in its calculation. Here, $\psi_{iso}(y,\rho)$ was found to be robust to the number of density layers when it is 92 or higher (tests were performed with 184 layers, and a 7% or less L2 error was found for all four of the summer and winter experiments) .

$\psi_{iso}(y,\rho)$ in Eqn. (A2) is a function of density, not depth. Therefore it is convenient to remap it to height coordinatesin order to compare it to $\overline{\psi}$. Following the method of (Wolfe and Cessi, 2015), the remapping $\psi_{iso}(y,\rho) = \psi_{iso}[y,\overline{\rho}(y,z)]$ is used. In practice, first, the cumulative sum of the latidue-depth plane for convenience. The averaging is thus a time and zonally averaged layer thicknesses $\overline{H_\rho}(y,\rho)$ was taken, associating each density level with a single depth (which varies meridionally). This allows $\psi_{iso}(y,\rho)$ to be interpolated from the meridionally varying heights $\overline{H_\rho}(y,\rho)$ to the fixed vertical gridzonal-average in 3D (effectively time-average only in 2D) and eddies are departures from this average. The residual-mean overturning, $\psi_{iso}(y,z)$, is obtained first, by computing the overturning in density coordinates and remapping it to height coordinates, where it can be readily compared to the Eulerian overturning, $\overline{\psi}(y,z)$. The eddy induced overturning is then obtained as the difference between the residual-mean and the Eulerian overturnings, $\psi_{eddy} = \psi_{iso}(y,z) - \overline{\psi}(y,z)$. Comparison of overturnings components in simulations with and without eddies will shed light on the role of the SMLEs.

For For details of how ψ_{iso} is calculated with MITgcm outputs, see A2. For the 2D simulations, the streamfunctions ψ_{iso} and $\overline{\psi}$ are calculated in exactly are calculated the same way . They are as in the 3D simulations, and then scaled by a factor L_x so that their magnitudes are comparable can be compared to the 3D streamfunctions.

~~Finally, the difference between the $\overline{\psi}$ and ψ_{iso} is defined as the eddy-induced circulation ψ_{eddy} (Abernathey et al., 2011):~~

$$\psi_{eddy} = \psi_{iso}(y,z) - \overline{\psi}(y,z).$$

~~An equivalent way of writing this is thatthe total averaged layer transport has two components. First, there is the product of the individual averages of the meridional velocity and layer thickness $\overline{v}$ and $\overline{H_\rho}$~~Finally, ~~$\overline{vH_\rho}$. The second component is the eddy component $\overline{v'H'_\rho}$, the departure from the average. Overall we have $\overline{vH_\rho} = \overline{v}\,\overline{H_\rho} + \overline{v'H'_\rho}$, where the dash indicates departure from the time and zonal-average in 3D and time-average in 2D. Note that, because $\psi_{\rm eddy}$~~ note that, because ψ_{eddy} contains a departure from the time-mean component of the total circulation in both 2D and 3D simulations, it is sometimes referred to hereon as the transient component of the circulation. In particular, here, $\psi_{\rm eddy}$ includes the drift of system away from the initial conditions. This (small) contribution, which does not represent SMLEs, is noticeable in some simulations (see below).

3 Results

In this section, the results are discussed first for the Arctic summer experiment, starting with a description of the SMLE development~~and then going on to outline~~ , then the eddy impact on air-sea fluxes and sea ice, before describing the role of the eddy dynamics. Secondly, the results for the Arctic winter experiment are ~~given, in the same order. Next, Antarctic experiments are compared to Arctic ones, first summer and then winter~~ described (section 3.2). Sensitivity experiments to an Antarctic-like initial background stratification are discussed for summer and winter in section 3.3. Finally, results of the sensitivity of the eddy impact to MLD, atmospheric forcings and initial sea ice thickness are presented in section 3.4.

3.1 Arctic summer

3.1.1 Submesoscale eddy development near to the ice edge

In summer, the atmospheric forcing ~~generates a meridional density gradient in the ML due to the presence of sea ice over the northern half of the domain. The atmospheric forcing~~ drives ice melt and freshwater input ~~to the surface of the ice-covered ocean while the penetrating shortwave heating~~ in the northern half of the domain, while the shortwave radiation warms the open ocean faster than the ice-covered ocean. ~~Because the released freshwater is very buoyant and remains close to~~ The atmospheric forcing therefore generates a meridional density gradient in the ML. Within a few meters from the surface, the developing ML meridional density gradient is ~~salinity dominated near the surface~~ dominated by salinity as the released freshwater from ice melt is very buoyant (lighter water on the ice-covered ocean side~~) but~~ ; Fig. 2a). However, below this freshwater lens down to the bottom of the ML, the meridional density gradient is temperature-dominated~~(lighter water on~~ , with relatively warm water in the open ocean ~~side) from a few meters of depth to the bottom of the ML (Fig. (2a~~ , and near freezing temperatures in the ice-covered ocean (Figs. 2a and 3a)~~). A~~ . The MLD is defined using the default MITgcm surface-referenced density criterion. As a consequence of the ~~developing freshwater stratification close to the surfaceis that~~ spreading of the melt freshwater lens

near the surface, the MLD rapidly drops to a few metres in just a few days in both ice-free and ice-covered areas, though the ML remains weakly stratified below this (Fig. 3c).

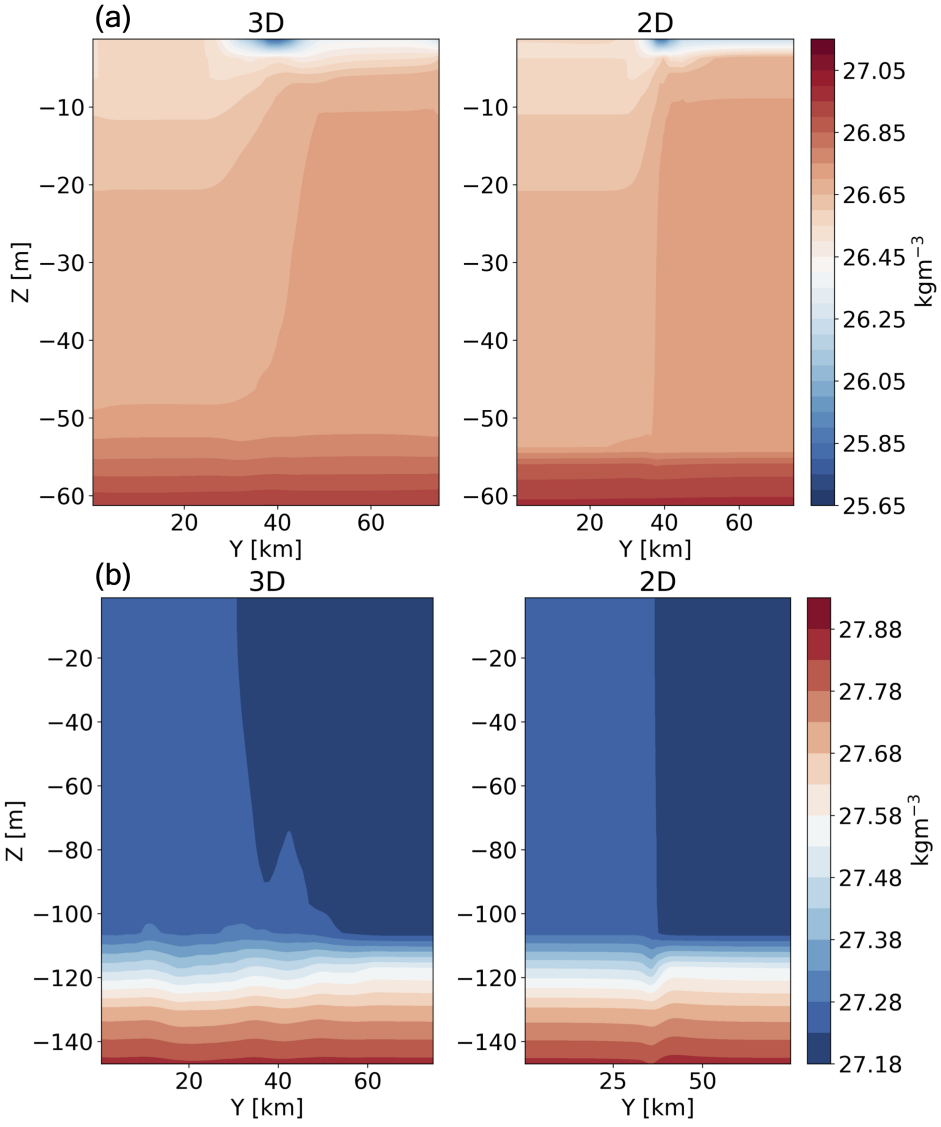

Figure 2. Snapshots of potential density (referenced at the surface) at day 50 of the 3D (zonal mean~~(~~, left) and 2D (right) simulations, for (a) Arctic summer (b) and Arctic winter.

Through ~~the ML~~ baroclinic instability, ~~ML eddies~~ SMLEs develop near the ice edge, where the meridional density gradient is the strongest. Fig. 4a displays the Rossby number~~for the summer simulation, clearly picking out~~ , clearly highlighting the SMLE vortices that have been energised through the ML instability. The Rossby number is on the border of the submesoscale

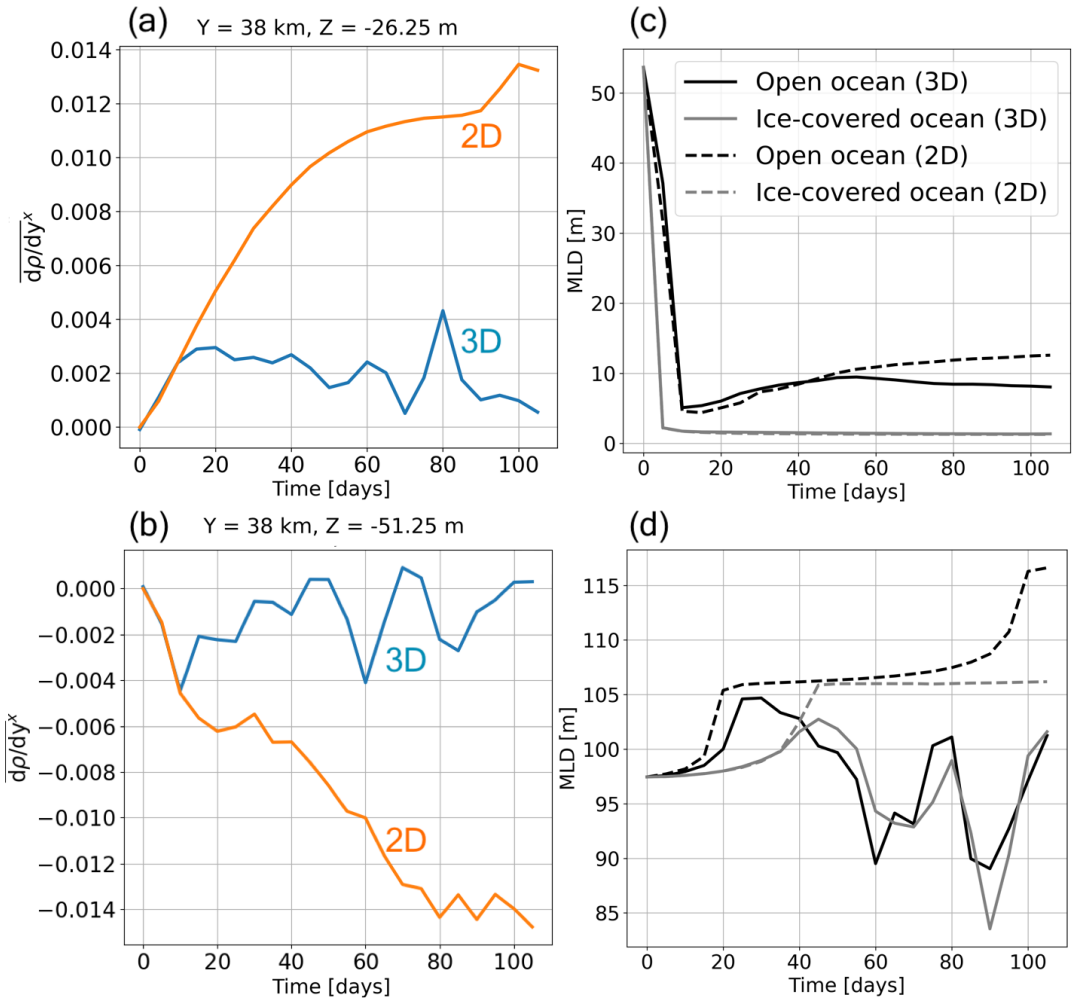

Figure 3. (a,c) Arctic summer, (b,d) Arctic winter. The left panel (a,b) displays the time evolution of the zonally averaged meridional density gradient in 2D and 3D simulations at $y = 38$ km, and $z = -26.25$ m (summer) and $z - 51.25$ m (winter). The right panel (c,d) displays the time evolution of ice-covered and open ocean spatially averaged MLDs for 3D (solid lines) and 2D (dashed lines) simulations.

range at $Ro \approx 0.3$. By day 50, eddies are well developed, as illustrated by a snapshot of SST (Fig. 4c). ~~Eddy filaments and vortices grow at the interface of relatively warm water in the open ocean and water at freezing temperature underneath the ice cover.~~ The vertical eddy buoyancy flux $\overline{w'b'}^{xt}$ (where prime denotes departure from the zonal mean, w is vertical velocity, and $b = \frac{-g\rho}{\rho_0}$ is buoyancy) is shown at the surface and at depth $z = -28.75$ m in Fig. 5a. The time average is taken over the whole simulation period of 110 days. If the vertical eddy buoyancy flux is positive (bringing light water up or dense water down), then the eddies act to restratify the ocean ML. As ~~mentioned~~described above, the meridional density gradient is dominated by salinity near the surface and temperature below the surface. Fig. 5a illustrates that 1) eddies do not reach the full meridional extent of the domain by the end of the simulation in summer, 2) at the surface (salinity dominated) the vertical eddy buoyancy

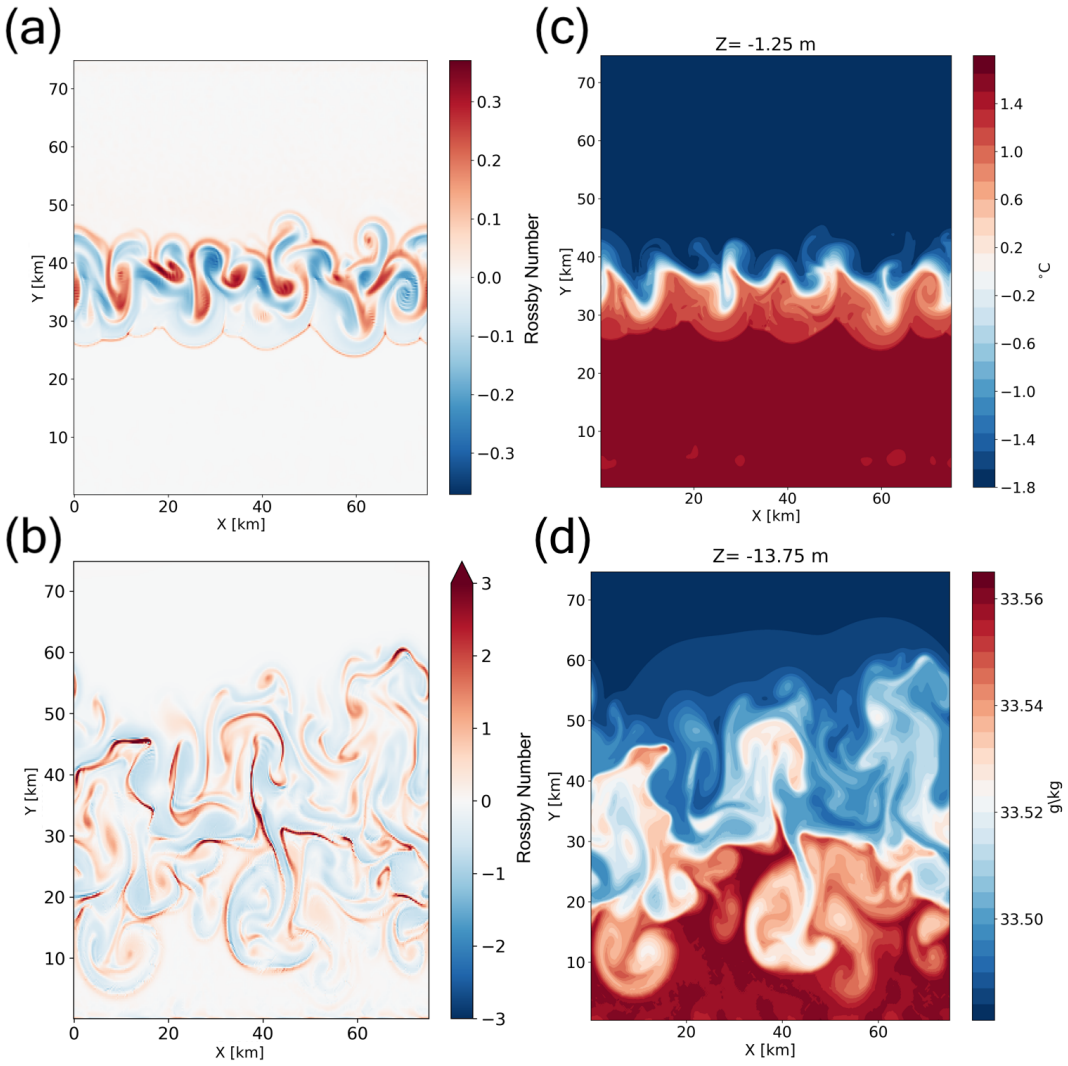

Figure 4. Snapshots of properties at day 50 for the Arctic case: (a,c) summer, (b,d) winter. The left panels (a,b) display the Rossby number ($=\frac{|\zeta|}{f}$) at the surface (note the differing colourbars). The top right panel (c) displays the sea surface temperature, and the bottom right panel (d) displays the salinity at a depth of $z = -13.75$ m.

flux can be negative (i.e., destratifying), and 3) below a few meters, it is strictly positive (i.e. restratifying) with the strongest effect near the ice edge. It is noteworthy that ~~, despite the MLD dropping to a few meters within days, the~~ the SMLEs extend over the full initial MLD of 55 m for the entire simulation despite the MLD dropping to a few meters within days (more details in section ~~??~~3.1.2). The ~~MLD is defined as the depth at which there is a significant vertical stratification, but the ocean is weakly stratified~~ weakly stratified ocean, from below the ~~MLD~~ freshwater lens down to 55 m depth, ~~hence it~~ remains prone to ML instability.

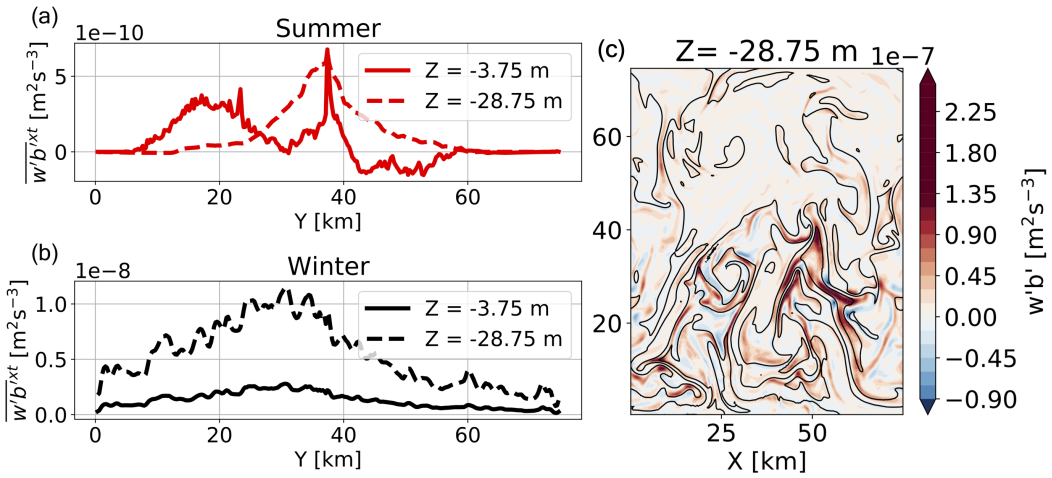

Figure 5. Time and zonal averages of vertical eddy buoyancy flux at the surface and at $z = -28.75$ m for (a) Arctic summer and (b) Arctic winter. The time average is taken over the full simulation length of 110 days. Note the different scales on the y-axis between a) and b). (c) spatial variations of $w'b'$ in the Arctic winter simulation at day 110, with salinity contours, spaced at 0.02 g kg^{-1}, shown in black.

The tendency of eddies to release available potential energy (PE), flatten isopycnals, and restratify the ML is therefore felt through the full depth of the initial ML. This is illustrated by comparing 2D and 3D density snapshots at day 50 (Fig. 2a). In the 2D run, the horizontal density gradient is more localised and stronger compared to that in the 3D run.

3.1.2 Eddy impact on air-sea heat flux and sea ice

To evaluate the role of eddies, it is useful to explore the heat budget of the ML. We ~~split~~ divide our domain into two boxes~~. The open ocean region extends~~ : an open ocean box from the southern solid wall to the middle of the channel ($Y_b = 38$ km) ~~. The equivalent region for the~~ and an ice-covered ~~ocean extends~~ box north of $Y_b = 38$ km. The two boxes extend from the ocean surface to a depth Z_b= 55 m (the summer initial MLD). For each of these regions of volume V, the volume-averaged ML heat budget in units of W m^{-2} is:

$$\underbrace{\rho_0 c_w Z_b \overline{\frac{\mathrm{d}T}{\mathrm{d}t}}^{xyz}}_{storage} = \underbrace{\overline{Q_{net}}^{xy}}_{surface} - \underbrace{\rho_0 c_w \overline{wT}\big|_{z=-Z_b}^{xy}}_{VHT} - \underbrace{(\frac{\rho_0 c_w Z_b}{Y_b})\overline{vT}\big|_{y=Y_b}^{xz}}_{MHT} + F_{diff.}, \quad (2)$$

where $\frac{\mathrm{d}T}{\mathrm{d}t}$ is the temperature tendency, c_w is the heat capacity of seawater, and Q_{net} is the total surface ocean heat flux. Overlines denote spatial averages. The advective terms are the vertical heat transport (VHT) and the meridional heat transport (MHT). Because the box depth captures the vertical extent of SMLEs (being the initial MLD of 55 m in summer), the VHT across the box bottom is negligible. $F_{diff.}$ are the net diffusive heat fluxes into the box. Q_{net} is ~~given by Eq. (1~~the net air-sea or ice-sea heat flux at the surface (see section 2.1).

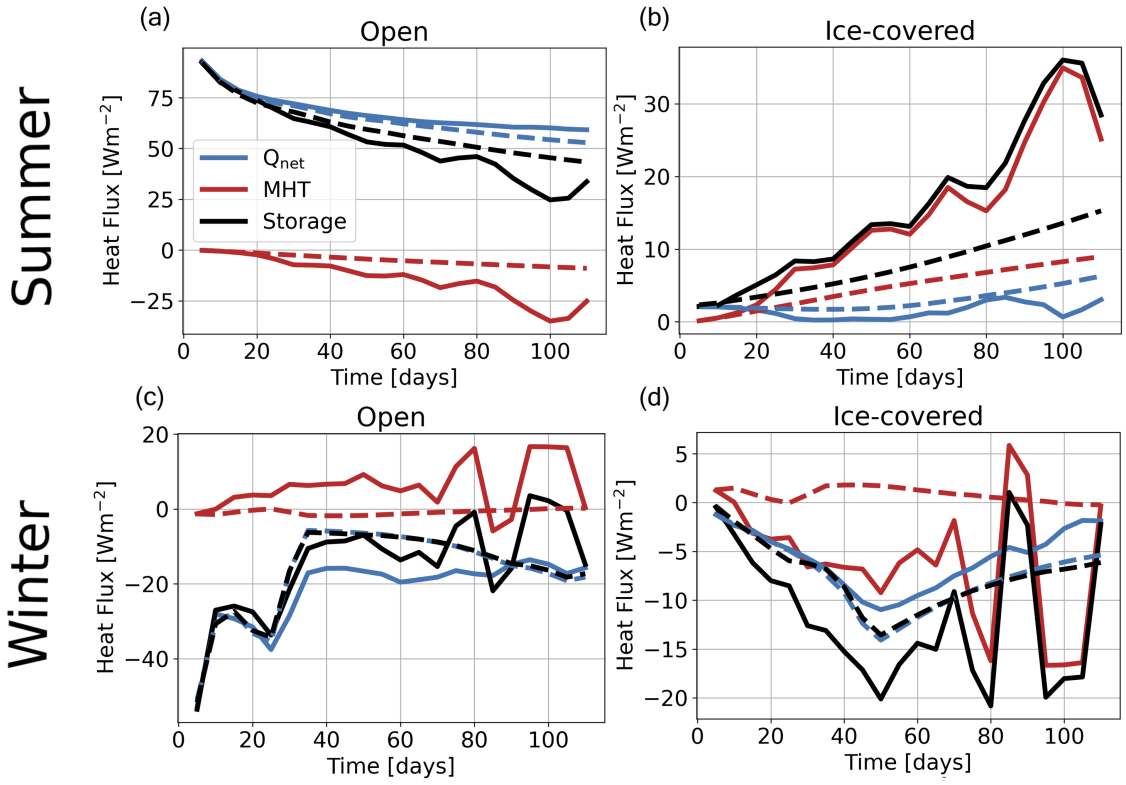

Figure 6. Top row: time evolution of Arctic summer open ocean (a) and ice-covered ocean (b) ML heat budgets. Bottom row: time evolution of Arctic winter open ocean (c) and ice-covered ocean (d) ML heat budgets. Solid and dashed lines denote the terms for the 3D and 2D simulations, respectively. For all quantities, 5-day averages are shown.

Under summer conditions, Q_{net} dominates the heat budget in the open ocean (Fig 6a). ~~The dominant terms in Q_{net} in the open ocean are the shortwave radiation, the sensible heat flux and the net longwave radiation.~~ Warming due to ~~$F_{SW,d}$~~ F_{SW} ($\mathcal{O}(10^2)$ W m^{-2}) dominates. However, the atmospheric temperature of approximately -10 °C brings about sensible cooling of the ocean ($\mathcal{O}(10^1)$ W m^{-2}), which increases in magnitude over time (from around 30 to 50 W m^{-2}) as the open ocean warms from (-1.8 °C to 3 °C). The increasing open ocean temperature also leads to a substantial increase in the magnitude of outgoing longwave radiation (-70 to -95 W m^{-2}). ~~Warming due to $F_{SW,d}$~~ Overall, steady warming due to F_{SW} ($\mathcal{O}(10^2)$ W m^{-2}) is partially ~~conpensated by a~~ compensated by (an increasing) cooling by F_{LWnet} and F_{SH}, leading to a decrease of Q_{net} over time (Fig. 6a).

~~The~~

The open ocean heat storage is mainly driven by Q_{net}, but with a significant contribution from MHT ~~.~~ (Fig. 6a). MHT (negative, pushing heat from the open ocean to the ice covered region) ~~reaches up to~~ peaks at -35 W m^{-2} in the 3D simulation, but only -9 W m^{-2} in the 2D simulation. This MHT is almost entirely due to the eddy-induced overturning. Fig. 7a shows

that the total overturning, ψ_{iso}, is dominated by ψ_{eddy}. ψ_{eddy} is maximum underneath the initial ice edge and extends from below the freshwater lens down to 50 m depth. As expected, ψ_{eddy} (clockwise) flattens the density front, by lifting lighter water on the open ocean side and pushing down denser water under the ice (i.e., removing the available potential energy that feeds baroclinic instability). Since density gradients over most of the initial MLD are temperature dominated, ψ_{eddy} realizes a northward MHT the ice-covered ML.

VHT indicates a small exchange of heat between the ML and the deeper ocean (around 1 W m^{-2}- not shown in Fig. 6). Vertical mixing terms were found to be negligible through the bottom boundary Z_b, and the surface correction term due to the linear free surface was also found to be negligible (not shown).

Overall, the open ocean heat storage decreases by almost half over the 110 days (from 90 to 40 W m^{-2}) as Q_{net} reduces over time and ~~MHT strengthens~~negative MHT strengthens in magnitude.

~~Now we consider the dominant heat budget quantities in the~~ In the ice-covered ocean region (Fig. 6b)~~. With ice~~, the net surface heat flux ~~Q_{net}~~ is almost 2 orders of magnitude smaller ~~than over the open ocean~~ (only a few W m^{-2}) ~~due to reflection and absorption by the ice~~than for the open ocean and changes little over time. All the heat flux components are much smaller in the ice covered region than in the open ocean as expected, but there are also compensating effects. As the ice cover melts and thins (due ~~mostly to in-situ~~ primarily to heating from shortwave radiation), ~~$F_{SW,d}$~~ and the fraction of open water in this region increases, F_{SW} into this region increases by an order of magnitude to $\mathcal{O}(10^1)$ W m^{-2}, but cooling via ~~$F_{LW\,net}$ and the~~ long-wave radiation and sensible heat flux also increases ~~when the ice cover melts leaving the open ocean surface. Overall the ice-covered Q_{net} changes little over time. Whilst the ocean surface temperature remains at the freezing point (as the surface~~ too. The resulting surface heating is balanced by ice melt~~such that the surface temperature changes only slightly~~ , maintaining the ocean surface temperature at the freezing point (only slightly increasing due to the salinity-dependence of the freezing point). However, the storage term over the full initial MLD in the ice-covered ocean is ~~positive, dominated by the MHT from the open ocean region, and indicates overall~~ overwhelmingly dominated by warming of the ML ~~especially~~ below a few meters~~at the surface~~, which is driven by the MHT from the open ocean region.

The impact of eddies on the heat budgets of both regions is observed by comparing the 3D and 2D results in ~~Figs~~Fig. 6(a,b). In the ice-covered region heat budget, by day 110, the MHT in the 3D simulation ~~reaches a time average of three times that of~~ is three times larger than in the 2D simulation~~by day 110. As a result, the time-averaged heat storage in the~~ , resulting in a storage twice as large in 3D ~~ice-covered region doubles compared to~~ than in 2D ~~by day 110~~ (compare red solid and dashed lines in Fig. 6b). This ~~demonstrates the large impact of eddies on the~~ can be traced back to the radically different streamfunctions in 2D compared to 3D (Fig. 7b). In 2D, there are no eddies and ψ_{eddy} is negligible (note that it is not exactly zero because of the transient component of the layer transport; see section 2.2). Therefore, in contrast to the 3D case, ψ_{iso} is approximately equal to $\overline{\psi}$. Interestingly, the latter is almost twice as large as in the 3D simulation, scaling with the stronger lateral density gradient in the 2D simulation. However, this is not enough to compensate for the negligible eddy-induced overturning, and overall the MHT from open ocean to ice-covered ~~region heat budget. An accelerated increase in ice melt occurs due to this~~ ocean is much larger with than without eddies.

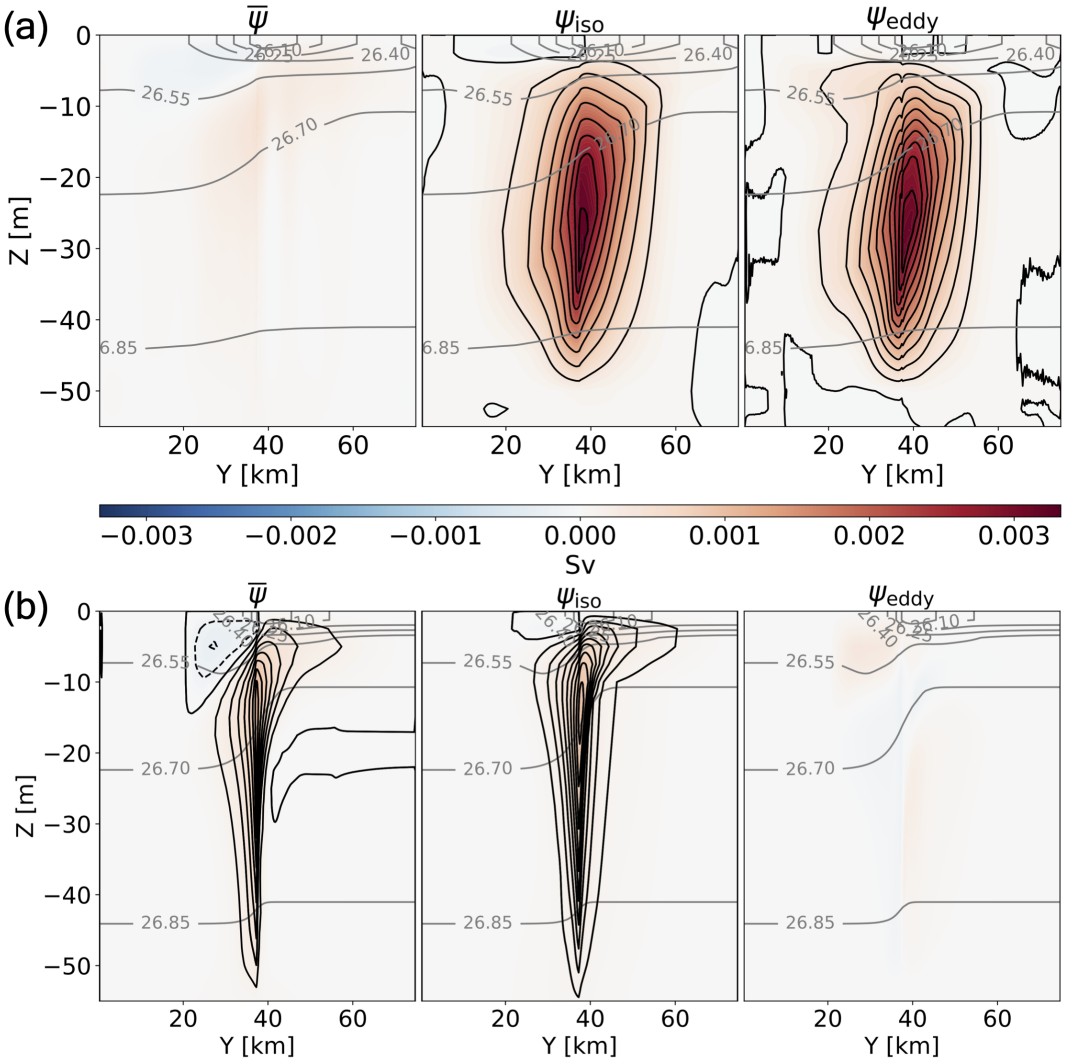

Figure 7. The Arctic summer time-averaged overturning stream functions for (a) 3D and (b) 2D simulations. $\overline{\psi}$ (left panels), ψ_{iso} (centre panels), and ψ_{eddy} (right panels). Red/blue shadings indicate clockwise/counterclockwise cells. Time-averaged isopycnals are shown in grey. The time period of averaging is the full simulation length of 110 days.

This increased eddy-induced ~~lateral heat transport under the ice~~MHT to the ice covered ocean supports a larger ice melt in 3D compared to 2D. The ice melt, in turn, impacts air-sea fluxes: a positive feedback is created between ice melt and ~~$F_{SW,d}$~~ F_{SW} as thinner and sparser ice coverage increases the fraction of ice-free ocean, and therefore the ML absorption of shortwave radiation ~~. On~~ (on average over the ~~time of the simulation, $F_{SW,d}$~~ simulation, F_{SW} is increased by 20% in 3D compared to 2D~~.~~). There is a partial cancellation of this effect by increased cooling by longwave radiation and sensible heat flux for that fraction, but shortwave radiation dominates.

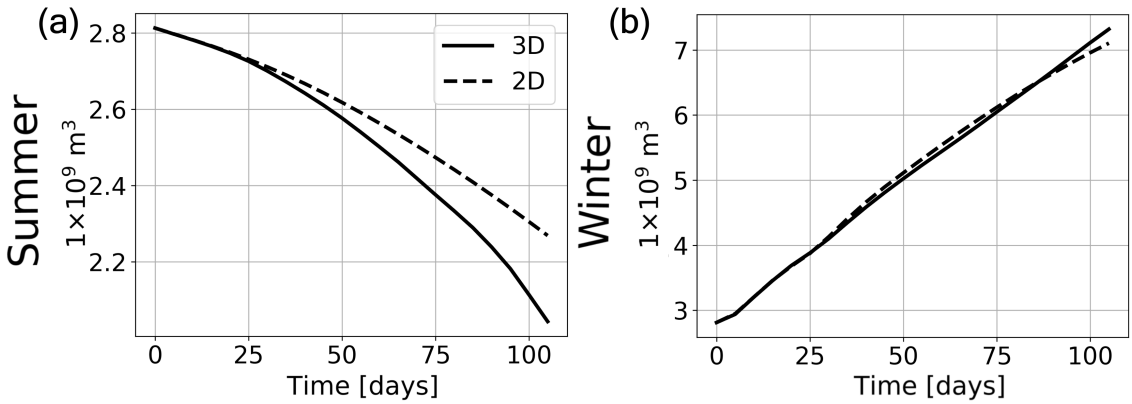

Figure 8. Total 3D (solid) and 2D (dashed) sea ice volume time series for (a) Arctic summer and (b) Arctic winter.

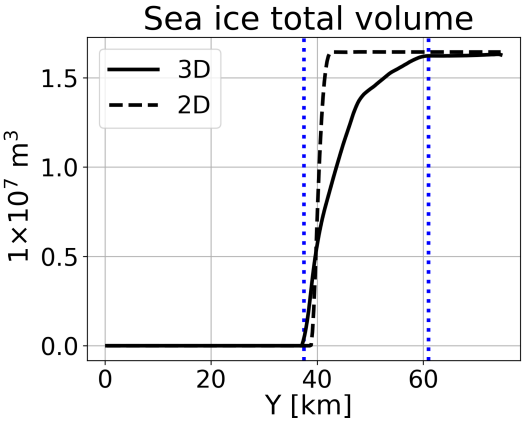

Figure 9. Day 110 snapshot of the zonal sum of sea ice volume, 2D and 3D Arctic summer (black lines). Blue ~~dashed~~ dotted lines ~~are an illustration of~~ indicate the meridional extent of the eddies (underneath the ice cover).

~~The~~ Comparing the time series of ~~total~~ sea ice volume ~~summed over the full domain for both~~ over the entire domain for 3D and 2D Arctic summer simulations ~~is shown in~~ shows the net large impact of the eddy heat transport on the ice cover (Fig. 8~~. For~~ a). We scaled up the 2D ~~, we scale up~~ timeseries by the number of zonal grid points in 3D ~~to obtain an equivalent volume~~for a meaningful comparison. The difference in total ice volume between the 2D and 3D simulations increases over time, reaching
330 ~~a total difference of~~ 10% by day 110. ~~However, this value of 10% is impacted by the region included in its calculation~~This metric, however, underestimates the impact of SMLEs, which is concentrated within the meridional extent of the eddies. Fig. 9 displays the sea ice volume at day 110 in 3D and 2D Arctic summer summed in the zonal direction. ~~The meridional extent of the eddies underneath the ice cover is shown by the blue dashed lines~~It emphasizes that the impact of SMLEs on sea ice is tightly linked to their spatial scale and growth rate. When only considering ~~the region bordered by these lines~~this region (bordered
335 by the blue dotted lines), the final 2D-3D sea ice volume difference rises to 17%~~(below we also consider the influence of the~~

choice of initial ice thickness on this number). Nonetheless, Fig. 9 emphasizes that the impact of SMLEs on the sea ice margin is tightly linked to their spatial scale and growth rate. In section 3.4, we also show that thinner initial ice cover leads to a much larger effect.

3.1.3 Eddy dynamics

The Arctic summer time-averaged overturning stream functions for (a) 3D and (b) 2D simulations. $\overline{\psi}$(y, z) (left panels), $\psi_{\rm iso}$ (centre panels), and $\psi_{\rm iso}$ (right panels). Red/blue shadings indicate clockwise/counterclockwise cells. Time-averaged isopycnals are shown in grey. The time period of averaging is the full simulation length of 110 days.

As in Fig. 7 but for Arctic winter. Note the different colorbar range compared to Fig. 7.

We now look more closely at the role of the SMLEs. In Fig. 7a, the clockwise direction of ψ_{eddy} indicates eddy-induced circulation acting to raise less dense (temperature-dominated density) water on the open ocean side and to sink denser water under the ice. As expected, the eddy-induced circulation acts to flatten the density front and feeds on the source of baroclinic instability, the available PE. ψ_{eddy} extends over the bulk of the ML below the ~5 m thick freshwater lens and is centred underneath the initial ice edge. The total overturning, ψ_{iso}, is dominated by ψ_{eddy}, and $\overline{\psi}$ is negligible in comparison. Fig. 7a demonstrates that the oceanic circulation, and associated heat transport to the ice-covered ML are largely due to the effect of eddies.

Fig. 7b (2D Arctic summer simulation) shows that the Eulerian overturning stream function associated with the density front is almost twice as large than in the 3D simulation, scaling with the stronger lateral density gradient in the 2D simulation. Furthermore, the total overturning ψ_{iso} in the 2D simulation is approximately three times smaller than ψ_{iso} in the 3D simulation. In 2D, there are no eddies, and $\overline{\psi}$ is approximately equal to ψ_{iso}. Note that ψ_{eddy} in 2D is negligible, but is not exactly zero, because of the transient component of the layer transport (see section 2.2). Nonetheless, this difference in ψ_{iso} between the 3D and 2D simulations corresponds well to the difference in magnitudes of the meridional heat transport between simulations displayed in the heat budget.

3.2 Arctic winter

3.2.1 Submesoscale eddy development near the ice edge

Like in summer, the winter initial conditions are horizontally uniform in temperature and salinity. Under winter atmospheric forcings, the ocean cools and ice forms within a few days. The rate of ice formation, which is associated with the rate of brine rejection, is faster in the open ocean, where ice is not already present or is thin. This is related to the conduction flux through ice which is inversely proportional to ice height. The salinity of the open ocean, therefore, increases faster than that of the ice-covered ocean (Fig. 4d). The developing winter ML density gradient (Fig. 3b) between the open and ice-covered regions is brought about by colder, saltier waters in the open ocean and warmer, fresher water in the ice-covered region (note that the density gradient is reversed compared to the summer case). AlsoThat said, the gradient is salinity dominated as the lateral temperature gradient is very small (ML is close to freezing point in both regions (the lateral temperature difference is less than

0.05 °C, compared to 3 °C in summer). This ~~is because the ML is close to freezing point in both regions~~also implies that eddy buoyancy fluxes (section 3.2.2) are not accompanied by significant lateral eddy heat fluxes in winter compared to summer. As a consequence of the ~~unstable ML, dense water is vertically mixed,~~ surface buoyancy loss, the ML deepens and warmer water is entrained from below the ML (Fig. 3d).

SMLEs develop through ML baroclinic instability near the sea ice edge as in the summer. Compared to the summer simulation, eddies develop and spread more rapidly, as well as reach higher Rossby numbers (Fig. 4b). The eddies spread heat and salinity anomalies laterally (Fig. 4d), extracting the available PE from the lateral density gradient. ~~Fig. 2b displays day 50 snapshots of potential density in 3D and 2D. Eddies develop and spread more rapidly, as well as reaching higher Rossby numbers, in the winter simulation compared to the summer simulation (Fig. 4b).~~ As expected, the ~~front is less steep in 3D than in 2D~~ density front is steeper (Fig. 2, lower panels) ~~, which is reflected in the evolution of density gradient in the two simulations~~ and grows sharper (Fig. 3b) in 2D than in 3D.

~~Fig. 5b shows the Arctic winter time~~

The time and zonal-mean vertical eddy buoyancy flux $\overline{w'b'}^{xt}$ ~~at the surface and at z =-28.75 m. $\overline{w'b'}^{xt}$ strengthens by~~ is an order of magnitude larger at depth (z =-28.75 m) than at ~~depth compared to at~~ the surface ~~, and at~~ (Fig. 5b). At both depths, ~~the~~ this restratifying flux is at least an order of magnitude greater than in summer (~~10^{-8} m^{2}s^{-3} at depth and 10^{-9} m^{2}s^{-3} at the surface~~compare the y-axis scale of Fig. 5a and Fig. 5b). This restratification (positive flux) by eddies opposes the destratifying influence of cooling and ice formation. In Fig. 5c, the winter spatial variations $w'b'$ are shown at day 110, with salinity contours shown in black. The alignment of $w'b'$ and salinity demonstrates that buoyancy anomalies are salinity dominated. $w'b'$ reaches up to 10^{-7} m^2 s^{-3} in parts of the open ocean, where air-sea fluxes are also larger. These magnitudes of vertical eddy buoyancy fluxes are equivalent to vertical heat fluxes (W m^{-2}) in the submesoscale range (Fox-Kemper et al., 2011; Fox-Kemper and Ferrari, 2008; Thomas et al., 2008).

3.2.2 Eddy impact on air-sea heat flux and sea ice

~~For the~~ As in the summer case, we investigate the heat budgets of the open ocean and ice-covered boxes. However, for the winter case, we set the bottom boundary of the ~~domains~~boxes, Z_b, at the approximate final MLD of 147 m. This is to ensure that all the SMLE dynamics are included within the heat budget.

The rapid onset of ice cover in the open ocean has a large influence on the time evolution of the winter heat budget (Fig. 6c). All winter heat budget terms other than the net surface heat flux, the MHT and the heat storage, are negligible and are not displayed in Fig. 6. In the open ocean, the initial net air-sea flux is -77 W m^{-2}. It stays at this value throughout the simulation at locations that remain ice-free (because it is controlled by the SST, which remains at freezing point). ~~At locations where~~ Where ice grows, the surface heat flux decreases to approximately -10 W m^{-2}. This explains the initial rapid reduction of the net surface heat flux averaged over the initially open ocean ~~(see in Fig. 6c,~~ from over -50 W m^{-2} to around -30 W m^{-2} (Fig. 6c). After around 40 days, Q_{net} is dominated by the presence of sea ice and changes little over the remaining 70 days of the simulation. The ice growth significantly affect all components of Q_{net}: F_{LWnet} (upwards) decreases from -120 to -82 W m^{-2} (with a small effect due to decreasing SST), F_{SH} decreases from -7 to -3 W m^{-2} and ~~$F_{SW,d}$~~ F_{SW} (downward) decreases by

~~just over~~ about one-half in 2D ~~and just under half in 3D (it ranges from 50 W m^{-2} into the open ocean to less than 10 W m^{-2} into ice-covered ocean).~~ on average. As in the summer case, Q_{net} is the dominant term in the heat budget in the open ocean region although with weaker values ($\mathcal{O}(10^1)$ W m^{-2}).

~~The ML open ocean heat storage term similarly remains large over time ($\mathcal{O}(10^1)$ W m^{-2}). This implies fast cooling of ocean waters below the base of the initial MLD (which are included in the heat budget volume average) through vertical mixing as the ML deepens. The temperature tendency near the ocean surface only~~ The temperature tendency over the top few metres of the ML is actually close to zero, because of the balance between ice formation, heat lost at the surface, and heat entrained from below the initial MLD. As mentioned above, the depth-averaged lateral temperature gradient is weak (and reversed) compared to the summer case~~at about -0.05 °C (+3 °C in summer)~~. As a result, the MHT acts to warm the open ocean, but it is smaller magnitude in winter than in summer.

In the ~~winter~~ ice-covered ocean region (Fig. 6d), the ice thickens over time in winter. Heat is conducted from the ocean through the ice and is lost to the atmosphere. Rates of ocean cooling (heat storage term) are lower than in the open ocean (by around 20 W m^{-2}) due to a complete and thicker ice cover. The heat storage term is dominated by the net surface heat flux Q_{net} and MHT in 3D (both cooling the ice-covered box), and only by Q_{net} in 2D. Again, the volume-averaged heat storage term also encompasses heat mixed upwards and lost at the surface, through the process of deepening the ML. ~~As in the winter open ocean region, the heat storage term nearer to the surface is much smaller due to the balance between heat loss through sea ice and entrainment of warmer water from below.~~

The MHT at the initial ice edge (Y_b =38 km) is small in 2D, less than 1 W m^{-2}, but up to 17 W m^{-2} in 3D. This ~~southward eddy-driven MHT acts to partially cancel the heat loss to the atmosphere that drives ML deepening in the open ocean, resulting in arresting MLD deepening there (see Fig. 3d). The eddy-driven cooling of the ice-covered ocean has a significant impact on the heat budget, reinforcing the heat loss through ice. The ML depth average heat storage in the ice-covered region decreases further, by around 30% on average over time, in 3D compared to~~ difference mainly reflects the difference in the magnitudes of the total streamfunction ψ_{iso} between 2D and 3D (Fig. ~~6d~~10).

~~The overall effect of the eddies on sea ice growth is however small. Eddies increase the total ice volume (over the whole domain) by only 3% by day 110. This is due to compensating effects. As more heat is transported laterally into the open ocean from under the ice in 3D than in 2D, less heat is obtained from below the ML in 3D, because eddies restratify and the ML does not deepen as much. Nearer to the ice edge, the balance between these lateral and vertical heat exchange terms is very fine, but further south the difference is more stark and the differences between the 2D and 3D sea ice volume are larger. In the ice-covered region, rates of surface heat loss and also basal heating are a smaller factor in the heat budget, so lateral eddy heat transport is more important for heat storage and ice formation rates. This means there is also higher ice growth and rates of heat loss in 3D in the winter ice-covered region.~~

3.2.3 ~~Eddy dynamics~~

~~The 3D and 2D Arctic winter overturning stream functions are displayed in Fig. 10(a, b), respectively. The 3D Eulerian streamfunction~~ As in the summer simulation, the Eulerian streamfunction is negligible (Fig. 10a, left) ~~is 2 orders of magnitude~~

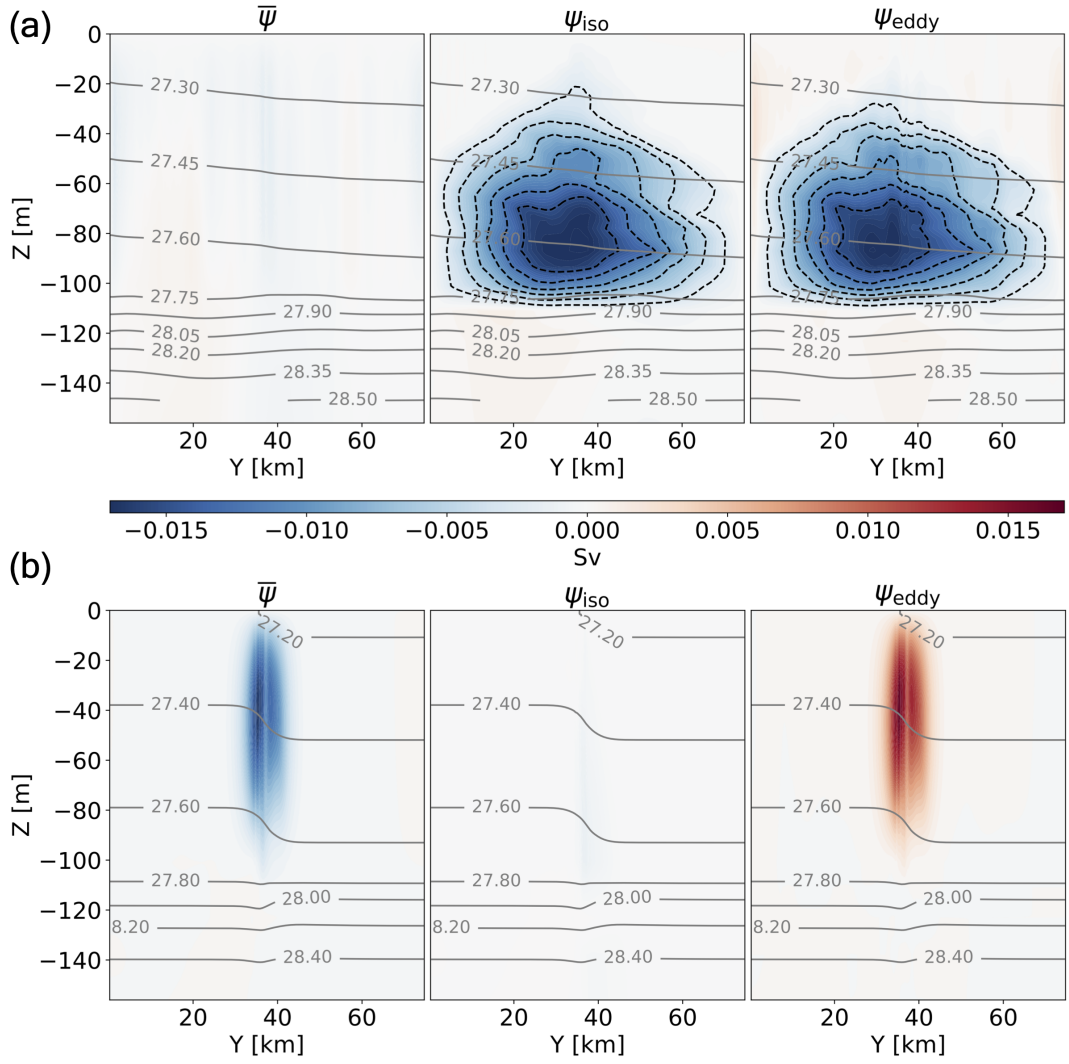

Figure 10. ~~Time evolution of difference~~ As in ~~MLD (zonally averaged) between simulations with eddies (3D) and no eddies (2D)~~ Fig. 7 but for ~~the~~ Arctic winter~~ease~~. Note the different colorbar range compared to Fig. 7.

~~less than ψ_{iso} and ψ_{eddy}, both of which are of order $\mathcal{O}(10^{-2})$ Sv. As in the summer simulation, the winter net~~ and the winter total overturning is dominated by the eddy dynamics in 3D. The ~~direction of the winter~~ eddy-induced overturning is ~~anticlockwise (opposite direction to the summer simulations, reflecting the reversed winter~~ now anticlockwise (reflecting the reversal of the lateral density gradient ~~). In the winter simulation, eddies~~ between summer and winter). Eddies act to drive fresher, warmer water ~~upwards~~ upward in the ice-covered region and cooler, saltier waters ~~downwards~~ downward in the open ocean region.

~~It is worth reiterating that, in~~ In 2D, where SMLEs are absent, only ~~time~~ temporal changes contribute to the eddy-induced overturning. ~~Fig. 10b shows that whilst~~ Whilst in summer this transient contribution ~~was negligible ($\overline{\psi}$ is approximately equivalent to ψ_{iso} in 2D)~~is negligible, in winter ~~the transient contribution is important . In particular,~~ it is important when averaged over the entire simulation ~~, the transient contribution is large~~ (but, again, by construction, it is zero when calculated instantaneously). ~~The 'ψ_{eddy}'~~ ψ_{eddy} in 2D is ~~positive~~ clockwise with a narrow meridional ~~extend. This transient component has a weakening impact on~~ extent. It is worth noting that, if this transient component exists in 3D, it would lead to an underestimation of the 3D eddy-induced overturning ~~(~~shown in Fig. 10a ~~, right), which would be stronger instantaneously. Overall the winter stream functions provide a helpful characterisation of the 3D eddy dynamics and confirm that~~(right). Nevertheless, as in the summer simulation, the total overturning ψ_{iso} in 2D (no eddies) is an order of magnitude weaker than in 3D.

The southward eddy-driven MHT acts to partially compensate the heat loss to the atmosphere that drives ML deepening in the open ocean, hence reducing MLD deepening there (see Fig. 3d). The eddy-driven cooling of the ice-covered ocean has a significant impact on the heat budget, reinforcing the heat loss through ice. The ML average heat storage in the ice-covered region decreases further, by about 30% on average over time, in 3D compared to 2D (Fig. 6d).

The overall effect of the eddies on sea ice growth is however small. Eddies increase the total ice volume (over the whole domain) by only 3% by day 110. This is due to compensating effects. As more heat is transported laterally into the open ocean from under the ice in 3D than in 2D, less heat is obtained from below the ML in 3D, because eddies restratify and the ML does not deepen as much.

Fig. 11 shows the time evolution of the difference in MLD between the 2D and 3D simulations (blue shading indicates deeper MLDs in 2D). The meridional expansion of the region with deeper 2D MLDs reflects eddies ~~travelling further~~ traveling farther away from the initial ice edge over time. Eddies reduce the deepening of the ML by 80% when averaged over the open ocean region and 52% when averaged over the ice-covered region by day 110. The difference between regions is because cooling and ML deepening are more rapid in the 2D open ocean region than in the ice-covered one. In both regions, the final 3D MLD is only 5 m deeper than the initial one, implying that eddies nearly balance the destratifying impact of atmospheric cooling and ice formation in both regions.

Nearer to the ice edge, the balance between these lateral and vertical heat exchange terms is very fine, but further south the difference is more stark and the differences between the 2D and 3D sea ice volume are larger. In the ice-covered region, rates of surface heat loss and also basal heating are a smaller factor in the heat budget, so lateral eddy heat transport is more important for heat storage and ice formation rates. This means there is also slightly higher ice growth and rates of heat loss in 3D compared to 2D in the winter ice-covered region. Overall, due to compensating eddy-induced MHT and VHT (though VHT in not displayed in Fig 6, since the box captures full depth of SMLE dynamics), the rates of sea ice growth are not significantly impacted by the presence of eddies in the winter experiment.

3.3 ~~Antarctic~~

3.3 Sensitivity to background stratification

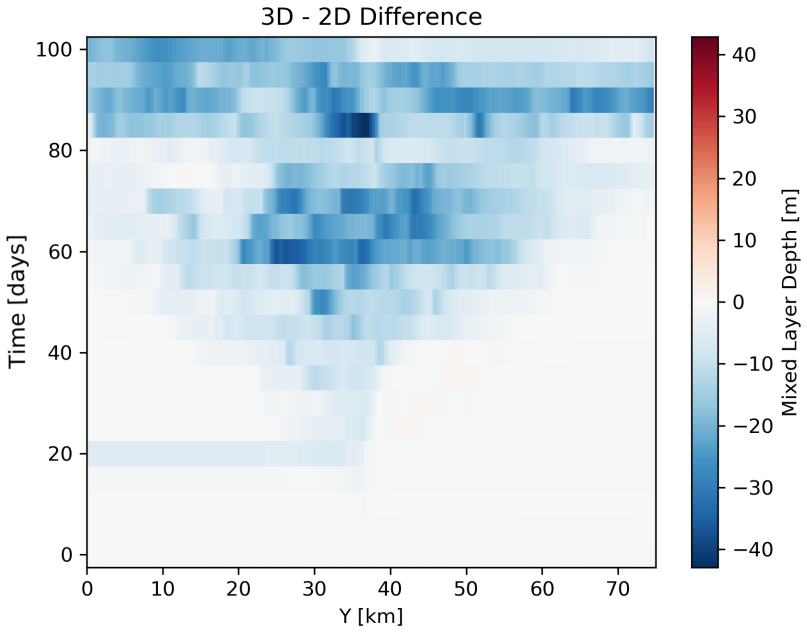

Figure 11. Time evolution of difference in MLD (zonally averaged) between simulations with eddies (3D) and no eddies (2D) for the Arctic winter case.

~~This section outlines the results for Antarctic summer and winter simulations, emphasizing how they differ from their Arctic counterparts. Initial~~

This section explores the sensitivity of the SMLEs impact to background stratification. To contrast with the stratification representative of the Arctic MIZ of the previous section, we use initial temperature and salinity profiles ~~used in the Antarctic simulations are displayed in~~ near the edge of the Antarctic sea ice cover, as described in section 2.1 and Fig. 1.

~~Ice-covered ML heat budgets for (a) Antarctic summer and (b) Antarctic winter (as in Fig. 6 but for the Antarctic simulations). Solid and dashed lines denote the 3D and 2D results, respectively.~~

3.3.1 Summer conditions

Under summer conditions, the ~~Antarctic initial stratification produces~~ Antarctic-like initial stratification results in only small differences in eddy impacts compared with the Arctic case. For example, eddies decrease the final ice volume by 11% with ~~Antarctic~~ Antarctic-like initial stratification, compared to 10% in the Arctic case. The MHT to the ice-covered region is only 4% larger for the ~~Antarctic than the Arctic~~ Antarctic-like 3D simulation on average ~~.~~ than for the Arctic case (Figs. 6b and 12a). The time-averaged open ocean heat storage, ice-covered ocean heat storage, and ~~ψ_{iso} exhibit negligible differences between~~ 3D ~~Arctic and Antarctic simulations~~ ψ_{iso} exhibited negligible differences for the two differing initial background stratitications

too. Therefore, eddies also have a significant impact on ~~the Antarctic summer~~ ice-covered region heat budget ~~, as illustrated in~~ with this change in initial background stratification (Fig. 12a).

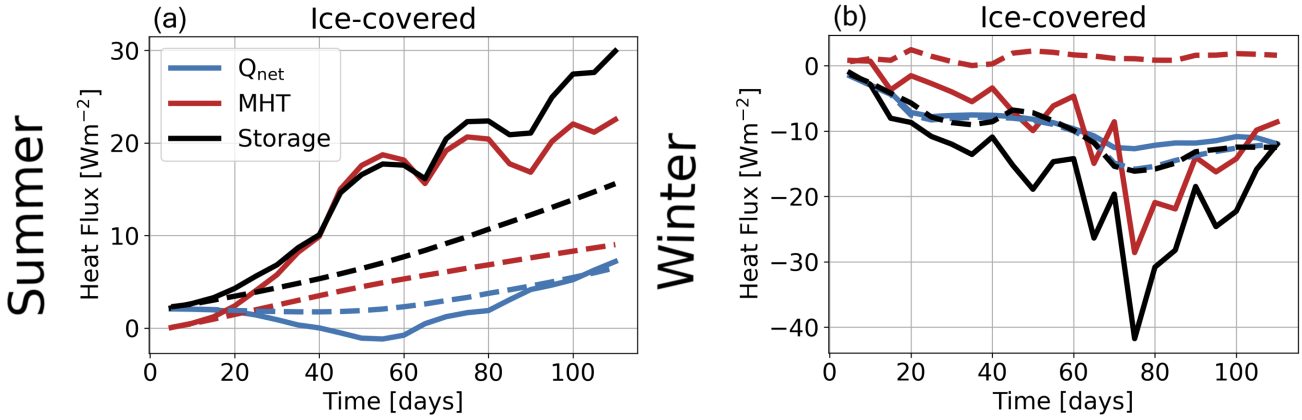

Figure 12. Ice-covered ocean ML heat budgets for (a) summer and (b) winter, (as in Fig. 6(b,d) but with initial Antarctic-like stratification rather than Arctic-like). As in Fig. 6, solid and dashed lines denote the 3D and 2D results with and without eddies, respectively.

This low sensitivity of the eddy impacts to initial ~~conditions in summertime~~ stratification in the summer conditions is due to the tendency of the summer atmospheric forcings to enhance ~~ML stratification in the ML~~ the upper ocean stratification and reduce the MLD abruptly. ~~This implies that there~~ There is little interaction between the ML and the subsurface ocean in the summer simulations. Therefore, the differences in stratification deeper than the initial MLD do not alter the eddy dynamics and impacts. ~~It is important to note that these findings may be limited by the simplifications of our model set-up. The simulations do not take into account the wind forcing, nor the difference in wind forcing between locations. A wind forcing would contribute to sustain the MLD against the restratifying effect of the surface buoyancy forcing, effectively reducing the strong decoupling we observe between the ML and the subsurface.~~

3.3.2 Winter conditions

~~In Antarctic winter, as the ML deepens,~~

Unlike in the summer case, the sensitivity to background stratification is significant in winter. This is simply because the ML deepens under winter forcing. The rate of vertical mixing and the heat from the subsurface ocean ~~is mixed upwards. The rate of vertical mixing depends~~ that is mixed upward depend on the strength of the stratification, which is weaker in the ~~Antarctic~~ Antarctic-like initial profiles than in the Arctic ~~ones. Fig. 13d displays~~ case. As a result, the rate of ML deepening ~~in the Antarctic simulations, which~~ with Antarctic profiles is significantly larger than ~~in the Arctic simulations (compare~~ with Arctic profiles (compare Fig. 13d with Fig. 3~~). In the Antarctic simulations, the~~ d). This also applies to the 2D case: rates of MLD deepening for the Antarctic-like stratification are over three times faster than in the Arctic (0.54 m/ day versus 0.16 m/ day). However, the 2D-3D differences are similar with the two background stratifications, about 10-15 m. For reference, the final

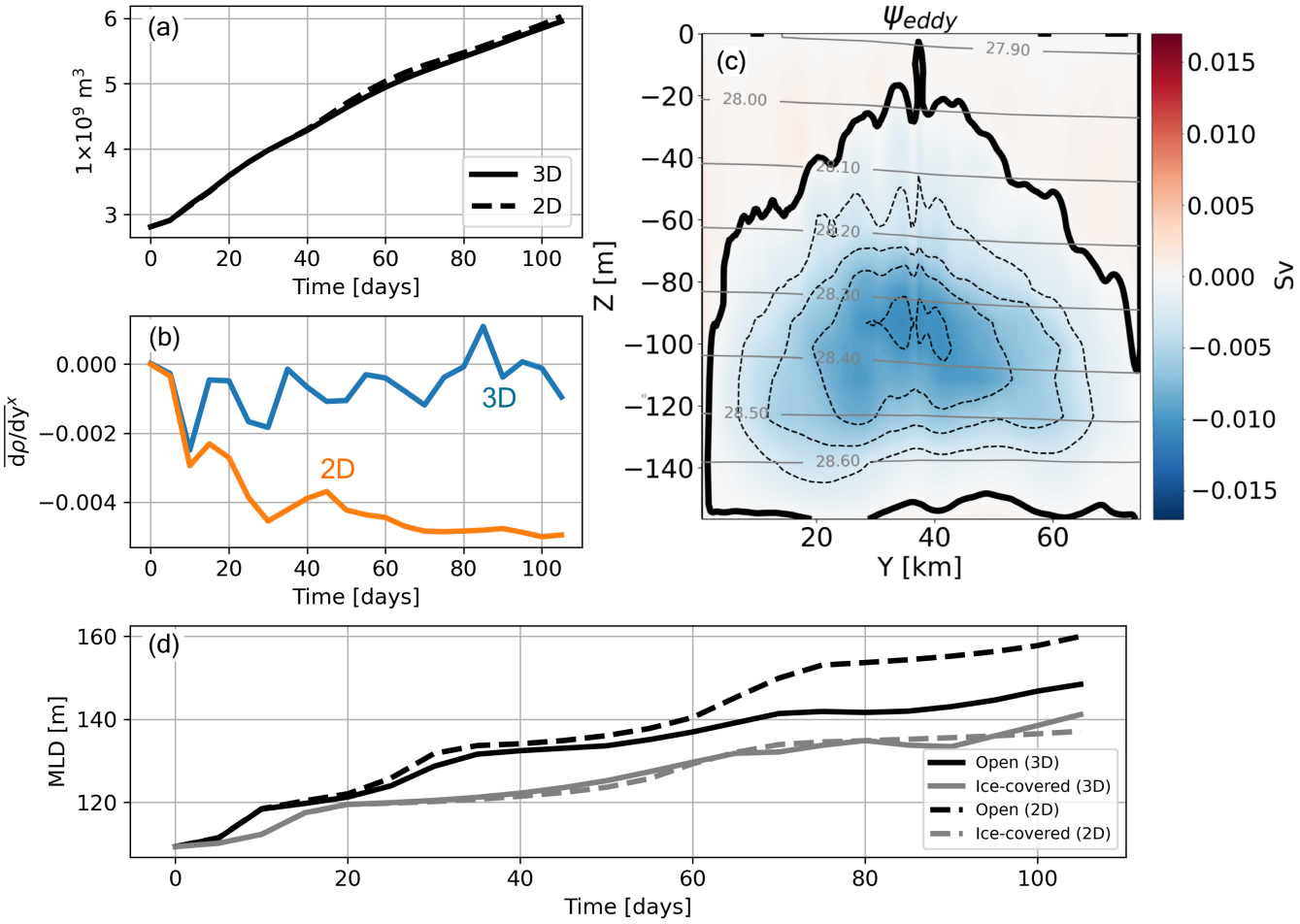

Figure 13. Results for the winter case with initial Antarctic-like stratification. (a) time evolution of total sea ice volume for both 3D (solid line) and 2D (dashed line) simulations (compare with the Arctic case in Fig. 8b). (b) time evolution of the zonally averaged meridional density gradient at y=38 km, and at z=-51 m (compare with Fig. 3b). (c) the 3D eddy-induced overturning (compare with Fig. 10a, right panel). (d) time series of MLDs for the open and ice-covered ocean (compare with Fig. 3(d)).

open ocean MLDs are approximately 160 m in 2D and 149 m in 3D ~~. In the Arctic simulations, they are~~ for the Antarctic stratification compared to 118 m in 2D and 103 m in 3D ~~(Fig. 3d). As in the Arctic simulations, the~~ for Arctic stratification. Using the 2D-3D difference in MLD ~~,~~ as a proxy for the strength of eddy restratification, ~~is greater in the open ocean~~ the effect is smaller in the ice-covered region than in the ~~ice-covered region . Notethat while eddies reverse the initial~~ open ocean region with both stratification profiles. Note, however, that eddies stop and reverse the MLD deepening in the Arctic winter simulation, ~~this does not happen in the Antarctic case because of the faster ML deepening , even if the total ML shallowing~~

effect by eddies is of the same magnitude for both locations (15 m for the Arctic and 11 m for the Antarctic simulations)but can only slow down the ML deepening with the weaker Antarctic stratification.

Results for the Antarctic winter case. (a) time evolution of total sea ice volume for both 3D (solid line) and 2D (dashed line) simulations (compare with the Arctic case in Fig. 8b). (b) time evolution of the zonally averaged meridional density gradient at y=38 km, and at z=-51 m (compare with Fig. 3(b)). (c) the 3D eddy-induced overturning (compare with Fig. 10(a), right panel). (d) time series of MLDs for the open and ice-covered ocean (compare with Fig. 3(d)).

The greater vertical mixing of heat upwards from the subsurface ocean in the Antarctic case that occurs with the Antarctic stratification results in a slower ice formation, and hence in weaker 3D and in 2-3 times weaker lateral density gradients compared to the Arctic case (Figs. 13b and 3b). The 2D lateral density gradientsgradient reaches $\sim$ -0.005 kgm^{-3}km^{-1}/$\sim$ -0.014 kgm^{-3}km^{-1} in the Antarctic/Arctic cases, respectively while the 3D gradients peak at $\sim$ -0.002 kgm^{-3}km^{-1} and $\sim$ -0.004 kgm^{-3}km^{-1} for the Antarctic/Arctic stratification, respectively. This effect can also be seen on the storage term in Fig. 12b, which is of greater magnitude in the Antarctic with the Antarctic-like stratification than in the Arctic simulationscase. That said, it is worth to note again that eddies have a small impact on sea ice cover in the winter simulations : by for both Antarctic-like and Arctic-like stratifications. By day 110, the 2D-3D difference in sea ice formation is -3% in the Arctic for the Arctic case, whilst it is +3% in the Antarcticwith the Antarctic-like stratification. Therefore, although there is faster MLD deepening and slower rates of ice formation overall (in both 3D and 2D) with the Antarctic-like stratification compared to the Arctic case, the eddy impact on sea ice formation (2D-3D difference) in winter is not altered by this change to the background stratification and remains small.

The Antarctic eddy-induced overturning stream function with the initial Antarctic stratification is overall deeper (stronger MLDdeepening) and (slightly) weaker than the Arctic one in line with a deeper MLD) but only slightly weaker than in the Arctic case (Fig. 13c). This is consistent with scalings from (Fox-Kemper et al., 2008), which predict a strengthening the eddy-induced streamfunction with the MLD and the lateral density gradient. The weaker lateral density gradient and larger MLD in the Antarctic case might partially cancel out leaving an eddy-induced streamfunction of similar strength to that of the Arctic case. A more quantitative comparison of our results with the parameterization of Fox-Kemper et al. (2008) is left to a future study.

3.4 Sensitivity to MLD, atmospheric forcings forcing, and initial sea ice thickness

Finally, in this section, we explore the sensitivity of the Arctic summer and winter experiments to different initial values of atmospheric forcingand MLDis explorededdy impact to atmospheric forcing, the initial MLD, and the initial sea ice thickness. More specifically, we test, for use the Arctic summer case , the sensitivity of the eddy impact on ice melt to different values of with values of the prescribed incoming shortwave radiation $F_{SW,d}$ (ranging from 180 to 270 W m^{-2}), of the initial MLD (from 10 to 100 m), and of the initial sea ice thickness (of 0.5 and 1 m). For Arctic winter, the sensitivity of the eddy impact is investigated for . In addition, we investigate initial MLD values of 55 to 155 m for Arctic winter case.

Fig. 14 summarizes the results Results of the sensitivity experiments . Fig. 14(a,b) display the Arctic summer 2D-3D percentage difference of final total sea ice volume for different values of $F_{SW,d}$ and different initial values of MLDare

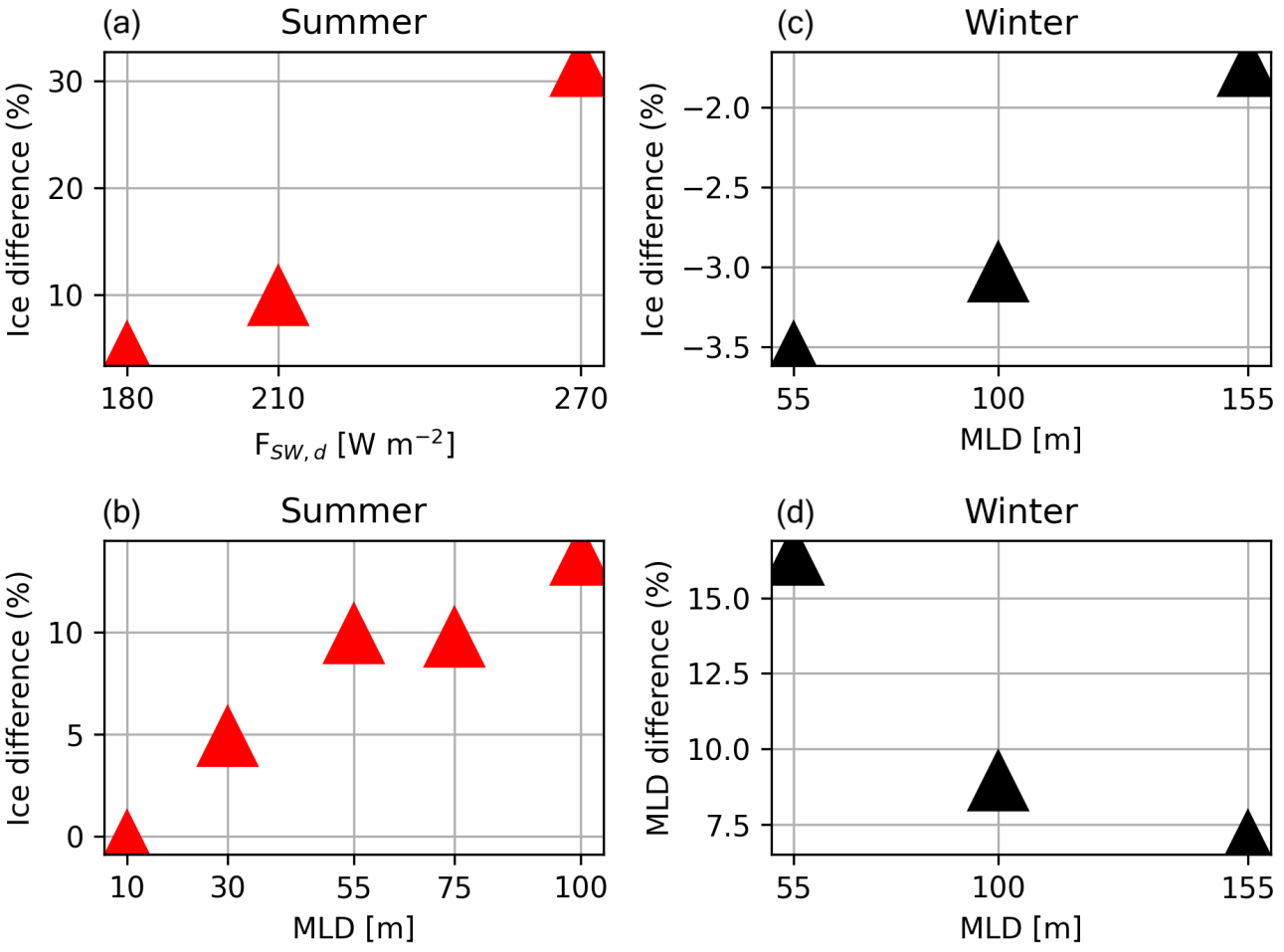

Figure 14. Sensitivity of Arctic summer 2D-3D ice volume difference to (a) $F_{SW,d}$ and (b) initial MLD. Sensitivity of Arctic winter 2D-3D ice volume difference (c) and 2D-3D difference in the final MLD (d), to the initial MLD. All quantities are spatially averaged.

summarized in Fig. 14. There is a near monotonic increase of the ~~eddy impact on sea ice for~~ 2D-3D difference of final total sea ice volume (in percent) with increasing $F_{SW,d}$ ~~or initial MLD~~ (panel a) initial MLD (panel b). The 2D-3D difference reaches 30% for $F_{SW,d} = 270$ W m^{-2} (due to stronger lateral density gradients and eddy MHT), and 14% for MLD = 100 m (again, due to stronger eddy overturning and associated MHT for deeper initial MLD).

~~Further~~Furthermore, when the initial ice thickness in the Arctic summer simulation is decreased from 1 m to 0.5 m, the 2D-3D percentage ice volume difference grows to 60%. ~~This demonstrates a strong dependence of the percentage impact of eddies on the initial ice thickness. Eddies actually melt about half as much ice overall in volume when the ice thickness is halved (the~~ In absolute volume, the eddy-driven melt (as measured by the 2D-3D final ice volume difference~~is about half when initial ice~~

volume is halved). However) with 0.5 m initial ice height is around half that with 1 m initial thickness, but represents a much larger fraction of the initial thickness. Additionally, melt due to non-eddy effects (e.g., positive shortwave radiation feedback) is much greater over time with a thinner ice cover. So the final ice volume in 2D with 0.5 m initial ice height is less than half the final ice volume in 2D with 1 m initial ice height. This means the eddy melt as a fraction of the 2D final ice coverincreases with 0.5 m initial ice height (even if in absolute volume the eddy melt is around half)initial ice cover.

For the Arctic winter case, Fig. 14c displays the sensitivity of the eddy impact on ice formation to the initial MLD. Unlike the summer case, the impact of eddies on the total amount of ice formed is not sensitive to the initial MLD. The percentage ice difference varies between 1.7-3.5% overall, effectively a doubling but this should be compared to a change from 0 to 15% in the summer case (panel b). Fig. 14d shows how the percentage difference in MLD due to eddies decreases as initial MLD is increased - the figure ranges from 16% with an initial MLD of 55 m to 7% with an initial MLD of 155 m. This reflects how the eddies do not proportionally restratify the ML by the same fraction with increasing MLD. Instead, the absolute reduction to MLD by eddies is almost constant for all tested initial MLDs, 10 ± 1.5 m.

4 Summary and discussion

In this study, the impact of submesoscale mixed layer eddies (SMLEs) generated near the sea ice edge on the ocean, sea ice and air-sea exchanges is explored using idealized numerical simulations. Our focus is on the thermodynamical coupling between SMLEs and sea ice, which has received little attention in previous studies compared to mechanical coupling (hence we do not consider the wind forcing).

We use submesocale-resolving simulations (at 250 m resolution) of the ocean mixed layer (ML) near the ice edge, representing a lead or the marginal ice zone. At the initial state, the northern half of the domain is covered with ice. 3D simulations with eddies are compared to 2D (no zonal variation, but otherwise identical) simulations where eddies are absent.

Four main experiments were used in order to To understand how SMLEs behave near the sea ice edge: , we consider ambient conditions (the initial temperature and salinity profiles, atmospheric conditions) representative of the Arctic and Antarctic marginal ice zone, summer and winter . Between locations, only the initial stratification differs, whilst, between seasons, the initial stratification, atmospheric forcings and initial conditions for both regions, different initial mixed layer depths(MLDs) differ. The season affects the sources of heat available to or accessed by the ML (i.e., atmosphere and subsurface ocean). Further sensitivity tests helped clarify the influence of these ambient conditions on our results. , and different initial sea ice thicknesses.

The key outcomes of our study are:

- The Arctic summersimulation shows that In summer, SMLEs energised near the ice edge have a leading order-to-moderate impact on air-sea heat exchange, ocean heat storage and lateral heat transport. In summer, although the ML shoals over time, the initial MLD (55 m) sets the vertical extent of the SMLEs and hence of the eddy-induced overturning, and this extent does not change over the simulation. The eddies have little influence on MLD but still act to increase

stratification over the full 55 m depth near the ice edge and under the ice, as well as restratifying near the surface through eddy transport of freshwater to the open ocean.

- Initially, open ocean storage rates are close to order 10^2 W m^{-2}, nearly 2 orders of magnitude greater than in the ice-covered region. This heat reservoir is efficiently made available to the ice-covered ocean by eddies; the rate of northward heat transfer is 3 times larger with than without eddies. When eddies are present (3D versus 2D), the net surface heat flux in the open ocean is 12% greater and the shortwave absorption in the ice-covered region increases by 20%.

- Effectively, eddies act as a heat pump: taking heat out of the atmosphere to move it under the sea ice laterally, which in turn accelerates the melting of sea ice. The northward heat transfer is 3 times larger with than without eddies. This creates a positive feedback with an increase in shortwave absorption over the thinner ice. Comparing the 3D and 2D simulations shows that , in about 3 months, We estimate that eddies contribute a further decrease of the ice volume of 17% in the region where they are present. This effect is strongly sensitive to the solar forcing and thickness of the initial ice cover. The percentage triples when the solar forcing increases from 180 W m^{-2} to 270 W m^{-2} or increases even more when the initial ice cover decreases from 1 to 0.5 mranging from 10 to 60% depending on initial and boundary conditions.

- In Under summer conditions, the Antarctic case shows a very similar behavior to the Arctic case. The background stratification(i.e., location) has little influence on the simulations above results are not significantly affected by the initial stratification. This is because the ML shallows rapidly and, therefore, the subsurface stratification does not influence the eddy development.

- In winter, we find a radically different situation. The heat lost to the atmosphere over the open ocean is partially balanced by heat stored below the ML (as the ML deepens) and by heat transported by eddies from the ice-covered region. Because of the restratifying effect of eddies, less heat is transferred upwards into the ML from the subsurface ocean in 3D than in 2D. In the Arctic winter simulations, eddies have a leading order impact on MLD, reducing the ML deepening by 80% or approximately 15 m. In the Antarctic, the reduction of deepening is similar to that of the Arctic ($\sim$ 11 m) but the percentage difference in final MLDs is smaller ($\sim$18%) due to larger initial MLDs.

- In winter, the direction of direction of the eddy-induced overturning is opposite and at least an order of magnitude larger than in summer, with a faster pace of eddy growth and subsequent transport of density anomalies. This is consistent with an eddy growth rate proportional to the MLDML depth (MLD), which is larger in winter. However, the eddy-induced MHT meridional heat transport is weaker than in summer because of the smaller meridional temperature gradient between regions (both at the freezing point). The eddy-induced meridional heat transport is nonetheless significant as the impact of eddies on air-sea fluxes in winter is of similar magnitude to that in summer.

- There are therefore In winter, there are two competing eddy effectsin winter: with eddies, less heat is transported from below the ML, transferred upward into the ML from the subsurface ocean (ML deepening due to atmospheric forcing and

ice formation is reduced, by about 10-15 m, with eddies due to their restratifying effects), but more heat is transported laterally by eddies from the ice-covered ocean. The former effect is marginally greater than the latter and so the net effect of eddies is to slightly increase ice growth in the open ocean region.

~~SMLEs~~

It is important to note that these findings may be limited by the simplifications of our model set-up. The simulations do not take into account the wind forcing. For example, a wind forcing would contribute to sustaining the MLD against the restratifying effect of the surface buoyancy forcing, effectively reducing the strong decoupling we observe between the ML and the subsurface in summer conditions. Other differences (such as sea ice characteristics, atmopsheric forcing, and topographic constraints) could influence these results and enhance the differences between Arctic- and Antarctic-like experiments. Also, using a simple sea ice model (and our focus on thermodynamic interactions) implies that we did not consider processes such as dynamics of ice floes, which have been shown to interact strongly mechanically with submesoscale eddies (e.g. Horvat et al., 2016; Gupta a . To move toward understanding of the real system, future work should aim to explore feedbacks between these effects. This may be particularly important for the improvement or design of submesoscale parameterization for polar regions.

For the near future, including SMLEs in climate models will rely on effective parameterizations capturing key behaviors. SMLEs are important for polar regions as well as globally due to the way they regulate heat exchange between the atmosphere and the deeper ocean (Thompson et al., 2016). Including these eddies in climate models can have significant impacts on sea ice cover, global heat budgets, air-sea exchange, and nutrient transport (Su et al., 2018; Fox-Kemper et al., 2011; Mahadevan, 2016). In addition, capturing SMLEs can energise mesoscale eddies at the larger scale and global ocean currents such as the AMOC (Lévy et al., 2012; Fox-Kemper et al., 2011).

~~Including eddies in climate models relies on effective parameterisations capturing key behaviours. This work helps to understand the impact of SMLEs in polar environments, and will aid with the development of SMLE parameterisations suitable for polar regions.~~

~~Specifically, an~~

An intriguing finding of our ~~simulations~~ study potentially relevant to parameterization is that the vertical scale of the eddies ~~and~~ (and hence the eddy-induced circulation) is primarily set by the initial MLD. ~~Even in summer , where the MLD drops to a few meters in days, the eddies keep the~~ In summer in particular, as the ML shoals to 5 m within weeks, SMLEs retain the memory of the initial MLD (~~∼50~~55 m) ~~while in winter~~over 110 days. The eddies have little influence on MLD but still act to increase stratification over the full 55 m depth. In winter, the eddy-induced overturning extends slightly over time to match the final MLD (from 100 to 150 m for the experiment with Antarctic-like stratification). This suggests a significant decoupling from or lag (∼month) of the eddy-induced overturning behind the MLD in summer. The Fox-Kemper SMLE parameterization (Fox-Kemper et al., 2008; Fox-Kemper and Ferrari, 2008; Fox-Kemper et al., 2011; Calvert et al., 2020) is currently the most used SMLE ~~parametrization~~ parameterization in climate models. Although this parameterization was not developed in the context of polar regions, it is regularly used in global set-ups, hence the need to evaluate its performance near the ice edge. Ongoing work explores the capabilities of the Fox-Kemper SMLE parameterization to capture the behaviour we have uncovered (to be published).

Overall, we have demonstrated that the thermodynamic SMLE-sea ice interaction leads to varying, up to leading order impacts of SMLEs on heat budgets, MLDs and sea ice cover of partially ice-covered regions. We have also shown that the impacts and mechanisms of SMLE impacts vary greatly with seasons. Finally, we have shown that the background conditions (stratification, sea ice thickness, forcing, MLD) can buffer or amplify these impacts.

Code availability. The MITgcm code and inputs needed to reproduce our results are provided in Greig and Ferreira (2025).

Appendix A

A1 ~~Initial conditions~~~~The horizontal eddy viscosity~~ Model set-up

The horizontal grid spacing for the MITgcm set-up is ~~set in both winter simulations to~~ 250 m and the vertical grid spacing is 2.5 m over the top 75 m. Below this, the vertical grid spacing increases by 20% at each subsequent grid point to a total depth of 538 m. A thermodynamic sea ice package is used, such that the sea ice advection by the ocean is switched off. In addition, there is a free-slip boundary on the ice-ocean interface. The northern horizontal extent of the domain is initially covered with 1 m thick sea ice, and the southern half is open ocean. Further, there is no wind forcing. An atmospheric boundary model evolves the atmospheric temperature in response to air-sea/air-ice fluxes (Deremble et al., 2013). There is no evaporation or precipitation between ocean and atmosphere.

Vertical mixing is represented by the K-profile parameterization mixing scheme (Large et al., 1994). Under summer conditions, a Smagorinsky viscosity scheme is used, with the Smagorinsky scaling coefficient set to 2. In winter conditions, vertical mixing and vertical velocities are much more intense than in the summer due to the large surface buoyancy loss (e.g., sensible heat loss, brine rejection). This requires higher viscosity to maintain numerical stability. To avoid damping all motions, we employed a horizontal eddy viscosity of 50 $m^2\ s^{-1}$ on the divergent component of the flow and ~~to 50~~of 1 $m^2\ s^{-1}$ on the ~~vorticity~~ rotational component of the flow ~~. In summer Smagorinsky viscosity scheme is used, with coefficient set to 2. In~~ in the winter simulation. In addition, a small horizontal diffusivity of 1 $m^2\ s^{-1}$ ~~was~~ is also used in winter simulations. These values were selected (a higher horizontal viscosity on the divergent part of the flow $\frac{\partial v}{\partial y}$ and a lower viscosity on the rotational component of the flow $\frac{\partial u}{\partial y}$) to decrease grid point noise, correlated to sea ice formation, on the meridional velocity field whilst not dampening the zonal jet. Sensitivity tests were conducted and these values were found to be the best for this purpose. To reduce the grid-point noise in the thermodynamic fields, the small amount of horizontal diffusion of temperature and salinity was introduced in the model. In addition, a third step to help with this issue was to change the smoothing settings within the KPP package. A few regularisations and smoothing options with the K-profile package were investigated. These include reducing the shear mixing when the velocity shear is low and the Richardson number is large. They helped to further reduce the noise in the velocity fields. In 3D we used the same values, whilst acknowledging this could potentially impact the development of SMLEs, by weakening the fronts.

A2 Calculation of the isopycnal stream function

The time-mean Eulerian Overturning Streamfunction (EOS) is calculated via zonal integration at a fixed height of the meridional velocity field:

$$\overline{\psi}(y,z) = -L_x \int_{H_d}^{z} \overline{v}(y,z')\mathrm{d}z', \tag{A1}$$

where H_d indicates the ocean bottom, L_x is the zonal extent of the domain, and $\overline{v}$ is the time and zonally-averaged meridional velocity field, which removes eddy effects.

Following Abernathey et al. (2011), the isopycnal streamfunction is defined as:

$$\psi_{iso}(y,\rho) = \int_{X} \int_{\rho_d}^{\rho} (vh)\mathrm{d}\rho'\mathrm{d}x, \tag{A2}$$

where $h = \frac{-\partial z}{\partial \rho}$ is a density layer thickness, ρ_d is the density of the deepest isopycnal, and ρ' is a dummy variable of integration.

Finally, the eddy-induced circulation ψ_{eddy} is obtained as the difference between $\overline{\psi}$ and ψ_{iso}:

$$\psi_{eddy} = \psi_{iso}(y,z) - \overline{\psi}(y,z). \tag{A3}$$

To calculate ψ_{iso}, the *layers* package in MITgcm is used. It calculates the layer transport $vH_\rho(x,y,\rho,t)$ online (at every time step), where $H_\rho(x,y,\rho,t)$ is the thickness of a density layer bin in metres (time averaging can be done later on). These density layer bins are chosen by the user at the start of the simulation. The full range of density bins chosen must cover the full range of ocean densities included in the simulation as well as their variation in time. $\psi_{iso}(y,\rho)$ in Eqn. (A2) is calculated by taking the cumulative sum of $\overline{vH_\rho}(y,\rho)$ (the sum was taken from the deepest isopycnal upwards). In this way, the meridional velocity v is integrated with respect to isopycnal layers rather than fixed vertical levels as in $\overline{\psi}(y,z)$. Ideally, $\psi_{iso}(y,\rho)$ should be robust to the choice of density bins used in its calculation. Here, $\psi_{iso}(y,\rho)$ was found to be robust to the number of density layers when it is 92 or higher (tests were performed with 184 layers, and a 7% or less L2 error was found for all four of the experiments).

$\psi_{iso}(y,\rho)$ in Eqn. (A2) is a function of density, not depth. Therefore it is convenient to remap it to height coordinates in order to compare it to $\overline{\psi}$. Following the method of Wolfe and Cessi (2015), the remapping $\psi_{iso}(y,\rho) = \psi_{iso}[y,\overline{\rho}(y,z)]$ is used. In practice, first, the cumulative sum of the time and zonally averaged layer thicknesses $\overline{H_\rho}(y,\rho)$ was taken, associating each density level with a single depth (which varies meridionally). This allows $\psi_{iso}(y,\rho)$ to be interpolated from the meridionally varying heights $\overline{H_\rho}(y,\rho)$ to the fixed vertical grid.

Author contributions. LG performed the analysis and led the writing of the manuscript at the University of Reading, UK. DF supervised, proposed and guided the project, and contributed to the writing and analysis.

Competing interests. The contact author has declared that none of the authors has any competing interests

Acknowledgements. LG was supported by the Centre for Doctoral Training in Mathematics of Planet Earth, with funding from the UK Engineering and Physical Sciences Research Council (EPSRC) (grant EP/L016613/1). We thank the authors of ~~(Horvat et al., 2016)~~ Horvat et al. (2016) for their code, which provided the basis for developing our set-up. Finally we would like to thank the two anonymous reviewers and the editor for their helpful comments, which improved the manuscript.

References

Abernathey, R., Marshall, J., and Ferreira, D.: The dependence of southern ocean meridional overturning on wind stress, J. Phys. Oceanogr., 41, 2261–2278, https://doi.org/10.1175/JPO-D-11-023.1, 2011.

Aylmer, J., Ferreira, D., and Feltham, D.: Different mechanisms of Arctic and Antarctic sea ice response to ocean heat transport, Clim. Dynam., 59, 315–329, https://doi.org/10.1007/s00382-021-06131-x, 2022.

Aylmer, J., Ferreira, D., and Feltham, D.: Impact of ocean heat transport on sea ice captured by a simple energy balance model, Nat. Commun. Earth Environ., 5, 406, https://doi.org/10.1038/s43247-024-01565-7, 2024.

Bitz, C. M., Holland, M. M., Hunke, E. C., and Moritz, R. E.: Maintenance of the Sea-Ice Edge, J. Climate, 18, 2903–2921, https://doi.org/10.1175/JCLI3428.1, 2005.

Brenner, S., Horvat, C., Hall, P., Lo Piccolo, A., Fox-Kemper, B., Labbé, S., and Dansereau, V.: Scale-Dependent Air-Sea Exchange in the Polar Oceans: Floe-Floe and Floe-Flow Coupling in the Generation of Ice-Ocean Boundary Layer Turbulence, Geophys. Res. Lett., 50, e2023GL105 703, https://doi.org/https://doi.org/10.1029/2023GL105703, 2023.

Calvert, D., Nurser, G., Bell, M. J., and Fox-Kemper, B.: The impact of a parameterisation of submesoscale mixed layer eddies on mixed layer depths in the NEMO ocean model, Ocean Model., 154, 101 678, https://doi.org/https://doi.org/10.1016/j.ocemod.2020.101678, 2020.

Cohanim, K., Zhao, K. X., and Stewart, A. L.: Dynamics of Eddies Generated by Sea Ice Leads, J. Phys. Oceanogr., 51, 3071–3092, https://doi.org/10.1175/JPO-D-20-0169.1, 2021.

Deremble, B., Wienders, N., and Dewar, W. K.: Cheapaml: A simple, atmospheric boundary layer model for use in ocean-only model calculations, Mon. Weather Rev., 141, 809–821, https://doi.org/10.1175/MWR-D-11-00254.1, 2013.

Docquier, D. and Koenigk, T.: A review of interactions between ocean heat transport and Arctic sea ice, Environ. Res. Lett., 16, 123 002, https://doi.org/10.1088/1748-9326/ac30be, 2021.

Fox-Kemper, B. and Ferrari, R.: Parameterization of mixed layer eddies. Part II: Prognosis and impact, J. Phys. Oceanogr., 38, 1166–1179, https://doi.org/10.1175/2007JPO3788.1, 2008.

Fox-Kemper, B., Ferrari, R., and Hallberg, R.: Parameterization of mixed layer eddies. Part I: Theory and diagnosis, J. Phys. Oceanogr., 38, 1145–1165, https://doi.org/10.1175/2007JPO3792.1, 2008.

Fox-Kemper, B., Danabasoglu, G., Ferrari, R., Griffies, S. M., Hallberg, R. W., Holland, M. M., Maltrud, M. E., Peacock, S., and Samuels, B. L.: Parameterization of mixed layer eddies. III: Implementation and impact in global ocean climate simulations, Ocean Model., 39, 61–78, https://doi.org/10.1016/j.ocemod.2010.09.002, 2011.

Frew, R. C., Bateson, A. W., Feltham, D. L., and Schröder, D.: Toward a marginal Arctic sea ice cover: changes to freezing, melting and dynamics, The Cryosphere, 19, 2115–2132, https://doi.org/10.5194/tc-19-2115-2025, 2025.

Giddy, I. S., Swart, S., Thompson, A. F., du Plessis, M., and Nicholson, S.-A.: Stirring of sea ice meltwater enhances submesoscale fronts in the Southern Ocean, Earth Space Sci. Open Arch., p. 43, https://doi.org/10.1002/essoar.10504395.1, 2020.

Giddy, I. S., Swart, S., Thompson, A. F., du Plessis, M., and Nicholson, S.-A.: Stirring of sea-ice meltwater enhances submesoscale fronts in the Southern Ocean, J. Geophys. Res.-Oceans, 126, e2020JC016 814, https://doi.org/https://doi.org/10.1029/2020JC016814, 2021.

Good, S. A., Martin, M. J., and Rayner, N. A.: EN4: Quality controlled ocean temperature and salinity profiles and monthly objective analyses with uncertainty estimates, J. Geophys. Res.-Oceans, 118, 6704–6716, https://doi.org/10.1002/2013JC009067, 2013.

Greig, L. and Ferreira, D.: Seasonal impact of submesoscale eddies on the ocean heat budget near the sea ice edge: code, https://doi.org/10.17864/1947.001447, 2025.

Gupta, M. and Thompson, A. F.: Regimes of Sea-Ice Floe Melt: Ice-Ocean Coupling at the Submesoscales, J. Geophys. Res.-Oceans, 127, e2022JC018 894, https://doi.org/https://doi.org/10.1029/2022JC018894, e2022JC018894 2022JC018894, 2022.

Haine, T. W. N. and Marshall, J.: Gravitational, Symmetric, and Baroclinic Instability of the Ocean Mixed Layer, J. Phys. Oceanogr., 28, 634 – 658, https://doi.org/10.1175/1520-0485(1998)028<0634:GSABIO>2.0.CO;2, 1998.

Hewitt, H., Fox-Kemper, B., Pearson, B., Roberts, M., and Klocke, D.: The small scales of the ocean may hold the key to surprises, Nat. Clim. Change 2022 12:6, 12, 494–503, https://doi.org/10.1038/s41558-022-01386-6, 2022.

Horvat, C. and Tziperman, E.: Understanding Melting due to Ocean Eddy Heat Fluxes at the Edge of Sea-Ice Floes, Geophys. Res. Lett., 45, 9721–9730, https://doi.org/10.1029/2018GL079363, 2018.

Horvat, C., Tziperman, E., and Campin, J.-M.: Interaction of sea ice floe size, ocean eddies, and sea ice melting, Geophys. Res. Lett., 43, 8083–8090, https://doi.org/https://doi.org/10.1002/2016GL069742, 2016.

Hosegood, P., Gregg, M. C., and Alford, M. H.: Sub-mesoscale lateral density structure in the oceanic surface mixed layer, Geophys. Res. Lett., 33, https://doi.org/10.1029/2006GL026797, 2006.

IPCC: Summary for Policymakers, in: Climate Change 2021 – The Physical Science Basis: Working Group I Contribution to the Sixth Assessment Report of the Intergovernmental Panel on Climate Change, p. 3–32, Cambridge University Press, https://doi.org/10.1017/9781009157896.001, 2023.

Large, W. G., McWilliams, J. C., and Doney, S. C.: Oceanic vertical mixing: A review and a model with a nonlocal boundary layer parameterization, Rev. Geophys., 32, 363–403, https://doi.org/https://doi.org/10.1029/94RG01872, 1994.

Lévy, M., Iovino, D., Resplandy, L., Klein, P., Madec, G., Tréguier, A. M., Masson, S., and Takahashi, K.: Large-scale impacts of submesoscale dynamics on phytoplankton: Local and remote effects, Ocean Model., 43-44, 77–93, https://doi.org/10.1016/j.ocemod.2011.12.003, 2012.

Mahadevan, A.: The Impact of Submesoscale Physics on Primary Productivity of Plankton, Annu. Rev. Mar Sci., 8, 161–184, https://doi.org/10.1146/annurev-marine-010814-015912, 2015.

Mahadevan, A.: The Impact of Submesoscale Physics on Primary Productivity of Plankton, Annu. Rev. Mar Sci., 8, 161–184, https://doi.org/10.1146/annurev-marine-010814-015912, 2016.

Manucharyan, G. E. and Thompson, A. F.: Submesoscale Sea Ice-Ocean Interactions in Marginal Ice Zones, J. Geophys. Res.-Oceans, 122, 9455–9475, https://doi.org/10.1002/2017JC012895, 2017.

Manucharyan, G. E. and Thompson, A. F.: Heavy footprints of upper-ocean eddies on weakened Arctic sea ice in marginal ice zones, Nat. Commun., 13, https://doi.org/10.1038/s41467-022-29663-0, 2022.

Marshall, J., Adcroft, A., Hill, C., Perelman, L., and Heisey, C.: A finite-volume, incompressible Navier Stokes model for studies of the ocean on parallel computers, J. Geophys. Res.-Oceans, 102, 5753–5766, https://doi.org/https://doi.org/10.1029/96JC02775, 1997a.

Marshall, J., Hill, C., Perelman, L., and Adcroft, A.: Hydrostatic, quasi-hydrostatic, and nonhydrostatic ocean modeling, J. Geophys. Res.-Oceans, 102, 5733–5752, https://doi.org/https://doi.org/10.1029/96JC02776, 1997b.

Matsumura, Y. and Hasumi, H.: Brine-driven eddies under sea ice leads and their impact on the Arctic Ocean mixed layer, J. Phys. Oceanogr., 38, 146–163, https://doi.org/10.1175/2007JPO3620.1, 2008.

McWilliams, J. C.: Submesoscale currents in the ocean, Proc. R. Soc. ARoyal Society A: Mathematical, Physical and Engineering Sciences, 472, 20160 117, https://doi.org/10.1098/rspa.2016.0117, 2016.

MITgcm contributors: MITgcm User Manual, Section 8.6.1.1.3: thsice, https://mitgcm.readthedocs.io/en/latest/phys_pkgs/thsice.html, accessed: 3 December 2025, 2025.

Munk, W., Armi, L., Fischer, K., and Zachariasen, F.: Spirals on the sea, Proc. R. Soc. ARoyal Society A: Mathematical, Physical and Engineering Sciences, 456, 1217–1280, https://doi.org/10.1098/rspa.2000.0560, 2000.

Purich, A. and Doddridge, E.: Record low Antarctic sea ice coverage indicates a new sea ice state, Nat. Commun. Earth Environ., 4, 314, https://doi.org/https://doi.org/10.1038/s43247-023-00961-9, 2023.

Rolph, R. J., Feltham, D. L., and Schröder, D.: Changes of the Arctic marginal ice zone during the satellite era, The Cryosphere, 14, 1971–1984, https://doi.org/10.5194/tc-14-1971-2020, 2020.

Shrestha, K. and Manucharyan, G. E.: Parameterization of Submesoscale Mixed Layer Restratification under Sea Ice, J. Phys. Oceanogr., 52, 419 – 435, https://doi.org/10.1175/JPO-D-21-0024.1, 2022.

Stroeve, J. C., Kattsov, V., Barrett, A., Serreze, M., Pavlova, T., Holland, M., and Meier, W. N.: Trends in Arctic sea ice extent from CMIP5, CMIP3 and observations, Geophys. Res. Lett., 39, https://doi.org/10.1029/2012GL052676, 2012.

Su, Z., Wang, J., Klein, P., Thompson, A. F., and Menemenlis, D.: Ocean submesoscales as a key component of the global heat budget, Nat. Commun., 9, 775, https://doi.org/10.1038/s41467-018-02983-w, 2018.

Swart, S., du Plessis, M. D., Thompson, A. F., Biddle, L. C., Giddy, I., Linders, T., Mohrmann, M., and Nicholson, S.: Submesoscale fronts in the Antarctic marginal ice zone and their response to wind forcing, Geophys. Res. Lett., 47, e2019GL086 649, https://doi.org/10.1029/2019GL086649, 2020.

Taylor, J. R. and Thompson, A. F.: Submesoscale Dynamics in the Upper Ocean, Annu. Rev. Fluid Mech., 55, 103–127, https://doi.org/https://doi.org/10.1146/annurev-fluid-031422-095147, 2023.

Thomas, L. N., Tandon, A., and Mahadevan, A.: Submesoscale Processes and Dynamics, in: Ocean Modeling in an Eddying Regime, pp. 17–38, AGU, https://doi.org/10.1029/177GM04, 2008.

Thompson, A. F., Lazar, A., Buckingham, C., Garabato, A. C., Damerell, G. M., and Heywood, K. J.: Open-ocean submesoscale motions: A full seasonal cycle of mixed layer instabilities from gliders, J. Phys. Oceanogr., 46, 1285–1307, https://doi.org/10.1175/JPO-D-15-0170.1, 2016.

Timmermans, M. L. and Winsor, P.: Scales of horizontal density structure in the Chukchi Sea surface layer, Cont. Shelf Res., 52, 39–45, https://doi.org/10.1016/j.csr.2012.10.015, 2013.

Timmermans, M. L., Cole, S., and Toole, J.: Horizontal density structure and restratification of the Arctic Ocean surface layer, J. Phys. Oceanogr., 42, 659–668, https://doi.org/10.1175/JPO-D-11-0125.1, 2012.

Vichi, M.: An indicator of sea ice variability for the Antarctic marginal ice zone, The Cryosphere, 16, 4087–4106, https://doi.org/10.5194/tc-16-4087-2022, 2022.

Winton, M.: A Reformulated Three-Layer Sea Ice Model, Journal of Atmospheric and Oceanic Technology, 17, 525–531, 2000.

Wolfe, C. L. and Cessi, P.: Multiple regimes and low-frequency variability in the quasi-adiabatic overturning circulation, J. Phys. Oceanogr., 45, 1690–1708, https://doi.org/10.1175/JPO-D-14-0095.1, 2015.